(12) INTERNATIONAL APPLICATION PUBLISHED UNDER THE PATENT COOPERATION TREATY (PCT)

(19) World Intellectual Property Organization
International Bureau

(43) International Publication Date
16 April 2020 (16.04.2020)

WIPO | PCT

(10) International Publication Number
WO 2020/076175 A2

(51) International Patent Classification:
Not classified

(21) International Application Number:
PCT/QA2019/050015

(22) International Filing Date:
08 October 2019 (08.10.2019)

(25) Filing Language: English

(26) Publication Language: English

(30) Priority Data:
62/744,414 11 October 2018 (11.10.2018) US

(71) Applicant: **QATAR FOUNDATION FOR EDUCATION, SCIENCE AND COMMUNITY DEVELOPMENT** [QA/QA]; PO Box 5825, Doha (QA).

(72) Inventor: **DEHBI, Mohammed**; c/o Qatar Foundation for Education, Science and Community Development, PO Box 5825, Doha (QA).

(74) Agent: **DEVSHI, Usha**; Qatar Financial Centre Branch licensed by the Qatar Financial Centre Authority (QFC No. 00144), Al Funduq Street, PO Box 26100 West Bay, Doha (QA).

(81) Designated States *(unless otherwise indicated, for every kind of national protection available)*: AE, AG, AL, AM, AO, AT, AU, AZ, BA, BB, BG, BH, BN, BR, BW, BY, BZ, CA, CH, CL, CN, CO, CR, CU, CZ, DE, DJ, DK, DM, DO, DZ, EC, EE, EG, ES, FI, GB, GD, GE, GH, GM, GT, HN, HR, HU, ID, IL, IN, IR, IS, JO, JP, KE, KG, KH, KN, KP, KR, KW, KZ, LA, LC, LK, LR, LS, LU, LY, MA, MD, ME, MG, MK, MN, MW, MX, MY, MZ, NA, NG, NI, NO, NZ, OM, PA, PE, PG, PH, PL, PT, QA, RO, RS, RU, RW, SA, SC, SD, SE, SG, SK, SL, SM, ST, SV, SY, TH, TJ, TM, TN, TR, TT, TZ, UA, UG, US, UZ, VC, VN, ZA, ZM, ZW.

(84) Designated States *(unless otherwise indicated, for every kind of regional protection available)*: ARIPO (BW, GH, GM, KE, LR, LS, MW, MZ, NA, RW, SD, SL, ST, SZ, TZ, UG, ZM, ZW), Eurasian (AM, AZ, BY, KG, KZ, RU, TJ, TM), European (AL, AT, BE, BG, CH, CY, CZ, DE, DK, EE, ES, FI, FR, GB, GR, HR, HU, IE, IS, IT, LT, LU, LV, MC, MK, MT, NL, NO, PL, PT, RO, RS, SE, SI, SK, SM, TR), OAPI (BF, BJ, CF, CG, CI, CM, GA, GN, GQ, GW, KM, ML, MR, NE, SN, TD, TG).

Published:
— *without international search report and to be republished upon receipt of that report (Rule 48.2(g))*
— *with sequence listing part of description (Rule 5.2(a))*
— *in black and white; the international application as filed contained color or greyscale and is available for download from PATENTSCOPE*

(54) Title: DIAGNOSIS, PREVENTION AND/OR TREATMENT OF CONDITIONS LINKED TO INSULIN RESISTANCE

(57) Abstract: Disclosed is a biomarker for diagnosis of a chronic condition linked to insulin resistance (IR) and a method of diagnosis using such a biomarker. The biomarker includes a polypeptide encoded by DNAJB3. The condition linked to IR can include diabetes, metabolic syndrome and their complications. A method of using the biomarker for diagnosis is also disclosed. A pharmaceutical composition including lipoic acid-α (ALA) can be used to prevent and/or treat a chronic condition linked to IR.

WO 2020/076175 A2

DIAGNOSIS, PREVENTION AND/OR TREATMENT OF CONDITIONS LINKED TO INSULIN RESISTANCE

PRIORITY

[0001] The present application claims priority to United States Provisional Application No. 62/744,414, filed October 11, 2018, the entire contents of which are being incorporated herein by reference.

BACKGROUND

[0002] Type 2 diabetes (T2D) is a multifactorial metabolic disorder that represents a major health, economic and social challenge worldwide. It is characterized by chronic hyperglycemia secondary to either increased insulin resistance (IR) in peripheral organs, progressive failure of the pancreatic islet β-cells or both (Defronzo RA, Diabetes 2009; 58: 773-795). The etiology of the disease is complex and involves an intricate interplay between genetic susceptibility and environmental factors, including sedentary lifestyles and obesity (DeFronzo, et al., Nature reviews Disease primers 2015; 1: 15019). This latter is recognized as a major independent risk factor for T2D through the development of IR (Upadhyay, et al., The Medical clinics of North America 2018; 102: 13-33).

[0003] Metabolic stress is a prominent hallmark underlying obesity, IR and T2D and it consists of a constellation of stress responses that are dysregulated in metabolically relevant sites. This includes chronic metaflammation (Hotamisligil G, Nature 2017; 542: 177-185), glucolipotoxicity (Poitout and Robertson 2008), increased oxidative stress (Houstis, et al., Nature 2006; 440: 944-948), mitochondrial dysfunction or biogenesis (Szendroedi, et al., Nature reviews Endocrinology 2011; 8: 92-103), and persistent ER stress (Engin and Hotamisligil, Diabetes, obesity & metabolism 2010;12 Suppl 2:108-115) with the concomitant impairment of the anti-inflammatory response (Pirola and Ferraz, World J Biol Chem 2017;8:120-128), anti-oxidant defense system (Picu, et al., Molecules (Basel, Switzerland) 2017; 22) and the heat shock response (HSR) (Abubaker, et al., PloS one 2013; 8: e69217; Rogers, et al., Diabetes 2016; 65: 3341-3351).

[0004] This metabolically toxic environment leads to a loss of homeostasis by activating several signaling pathways that abrogate the insulin action in insulin-responsive tissues

(Wellen and Hotamisligil, The Journal of clinical investigation 2005; 115: 1111-1119). Of these, the roles of c-Jun NH2-terminal kinase (JNK) stress kinase and the inhibitor of kappa B (IKKβ) inflammatory kinase in IR, β-cell dysfunction function and T2D are well established, and as such, they emerged as attractive therapeutic targets for obesity-induced IR and T2D (Arkan et al., Nature Medicine 2005; 11: 191-198; Hirosumi et al., Nature 2002 ; 420: 333-336; WO2O13/074986; EP2192200B1). At the molecular level, both enzymes interfere with the insulin action by phosphorylating the inhibitory serine of the insulin receptor substrate (IRS) and thereby, converting it to a poor substrate for the activated insulin receptor (Aguirre, et al., The Journal of biological chemistry 2000; 275: 9047-9054; Gao, et al., The Journal of biological chemistry 2002; 277: 8115-48121).

[0005] The HSR is a universal host-defense mechanism that plays a crucial role for cell survival under stressful conditions. This role is orchestrated by the immediate induction of a sub-set of highly conserved proteins called heat shock proteins (HSPs). HSPs were initially described as molecular chaperones involved in maintaining protein homeostasis by binding to misfolded and/or damaged proteins and assisting in their proper folding, disaggregation and remodelling (Saibil H, Nature reviews Molecular cell biology 2013; 14: 630-642). Subsequent studies demonstrated that some of the HSPs (i.e. HSP-25 and HSP-72) act as natural inhibitors of JNK and IKKβ kinases, and accordingly, they exhibit anti-apoptotic, anti-inflammatory and anti-oxidative stress properties (Park, et al., The EMBO journal 2001;20:446-456; Park, et al., The Journal of biological chemistry 2003; 278: 35272-35278; Simar, et al. Cell stress & chaperones 2012; 17: 615-621). Interventions that activate the HSR system are being intensively explored as alternative strategies to mitigate damages resulting from various stressful conditions including metabolic diseases.

[0006] DNAJB3 is a member of the heat shock protein-40 (HSP-40) cochaperone that was identified to be downregulated in the adipose tissue biopsies and PBMCs isolated from obese non-diabetic (Abubaker et al., PloS one 2013; 8: e69217) and diabetic (Abu-Farha, et al., Scientific reports 2015; 5: 14448) subjects, as well as in experimental animal model of high fat induced obesity (Aksu et al., J. Appl Genet 2007; 48: 133-143; Mitugi et al., Int J. Mol. Sci. 2015; 16: 14997-15008). Low levels of DNAJB3 were associated with enhanced metabolic stress and poor clinical outcomes (Abu-Farha et al., Scientific reports 2015; 5: 14448). Restoring the normal expression of DNAJB3 with a lifestyle intervention program (i.e., supervised physical exercise for at least 3 months) are associated improved outcomes (Abubaker et al., PloS one 2013; 8: e69217). Consistent with this, overexpression of DNAJB3

improved insulin signaling and glucose uptake in vitro in 3T3-L1 adipocytes (Abu-Farha et al., Scientific reports 2015; 5: 14448). More importantly, DNAJB3 interacts with both JNK1 and IKKβ kinases in co-immunoprecipitation assays (Abubaker et al., PloS one 2013; 8: e69217).

[0007] Increased IR in peripheral organs and progressive decline in β-cell function are the two early and crucial pathophysiological aberrations leading to chronic hyperglycemia and overt T2D. The etiology of the disease is complex and involves a complex interplay between genetic susceptibility and the negative health effects of a wide range of environmental and lifestyle factors, including high dietary fat content, physical inactivity, sedentariness and obesity (DeFronzo, R. A. *et al.* Type 2 diabetes mellitus. *Nature reviews. Disease primers* **1**, 15019, doi:10.1038/nrdp.2015.19 (2015)). Of these, obesity represents a significant contributing factor to T2D through the development of IR (Upadhyay, J., Farr, O., Perakakis, N., Ghaly, W. & Mantzoros, C. Obesity as a Disease. *The Medical clinics of North America* **102**, 13-33, doi:10.1016/j.mcna.2017.08.004 (2018)).

[0008] During the course of obesity, several stress/inflammatory pathways, with adverse effects on the insulin receptor signaling are activated in metabolically relevant tissues, leading to disruption of systemic metabolic homeostasis. Persistent ER stress, inflammatory response and enhanced oxidative stress together with defects in mitochondrial function, heat shock response (HSR) and the antioxidant defense system are the key hallmarks of IR and T2D. This metabolically toxic environment resulting from a titled balance toward the pro-stress state leads to the activation of several kinases; particularly JNK1 stress kinase and IKKβ inflammatory kinase, which phosphorylate IRS1 on specific inhibitory serine residues and results in impaired insulin-mediated downstream signaling. Therefore, therapeutic approaches that mitigate metabolic stress and promote the antioxidant and HSR have been proven to be effective in improving insulin sensitivity and glycemic control.

[0009] α-lipoic acid (ALA), also called thioctic acid or 1,2-dithiolane3-pentanoic acid is a naturally occurring dithiol compound enzymatically synthesized from octanoic acid in the mitochondria with a powerful antioxidant property. It acts as a crucial cofactor of the mitochondrial α-ketoacid dehydrogenase complexes involved in carbohydrate metabolism (Packer, L., Witt, E. H. & Tritschler, H. J. alpha-Lipoic acid as a biological antioxidant. *Free radical biology & medicine* **19**, 227-250 (1995)). Beside its primary role as a cofactor, ALA elicits other biochemical activities such as scavenging free radicals, regenerating the cellular antioxidant agents such as GSH, vitamin C and E, and modulating several critical signal transduction pathways (Packer, L., Witt, E. H. & Tritschler, H. J. alpha-Lipoic acid as a

biological antioxidant. *Free radical biology & medicine* **19**, 227-250 (1995); Rochette, L., Ghibu, S., Muresan, A. & Vergely, C. Alpha-lipoic acid: molecular mechanisms and therapeutic potential in diabetes. *Canadian journal of physiology and pharmacology* **93**, 1021-1027, doi:10.1139/cjpp-2014-0353 (2015); Rousseau, A. S. *et al.* alpha-Lipoic acid up-regulates expression of peroxisome proliferator-activated receptor beta in skeletal muscle: involvement of the JNK signaling pathway. *FASEB journal : official publication of the Federation of American Societies for Experimental Biology* **30**, 1287-1299, doi:10.1096/fj.15-280453 (2016); Solmonson, A. & DeBerardinis, R. J. Lipoic acid metabolism and mitochondrial redox regulation. *The Journal of biological chemistry* **293**, 7522-7530, doi:10.1074/jbc.TM117.000259 (2018); Yuan, Y. *et al.* Alpha-lipoic acid protects against cadmium-induced neuronal injury by inhibiting the endoplasmic reticulum stress eIF2alpha-ATF4 pathway in rat cortical neurons in vitro and in vivo. *Toxicology* **414**, 1-13, doi:10.1016/j.tox.2018.12.005 (2019)). ALA is a commonly used and readily available dietary supplement. In humans and experimental animal models, administration of ALA proved its pharmacotherapeutic value with a great therapeutic window index against several chronic diseases associated with metabolic stress such as diabetes (Rochette, L., Ghibu, S., Muresan, A. & Vergely, C. Alpha-lipoic acid: molecular mechanisms and therapeutic potential in diabetes. *Canadian journal of physiology and pharmacology* **93**, 1021-1027, doi:10.1139/cjpp-2014-0353 (2015); Ansar, H., Mazloom, Z., Kazemi, F. & Hejazi, N. Effect of alpha-lipoic acid on blood glucose, insulin resistance and glutathione peroxidase of type 2 diabetic patients. Saudi medical journal 32, 584-588 (2011); Derosa, G., D'Angelo, A., Romano, D. & Maffioli, P. A Clinical Trial about a Food Supplement Containing alpha-Lipoic Acid on Oxidative Stress Markers in Type 2 Diabetic Patients. International journal of molecular sciences 17, doi:10.3390/ijms17111802 (2016); Evans, J. L. & Goldfine, I. D. Alpha-lipoic acid: a multifunctional antioxidant that improves insulin sensitivity in patients with type 2 diabetes. *Diabetes technology & therapeutics* **2**, 401-413, doi:10.1089/15209150050194279 (2000); Jacob, S. *et al.* Enhancement of glucose disposal in patients with type 2 diabetes by alpha-lipoic acid. *Arzneimittel-Forschung* **45**, 872-874 (1995); Smith, J. D. & Clinard, V. B. Natural products for the management of type 2 diabetes mellitus and comorbid conditions. *Journal of the American Pharmacists Association : JAPhA* **54**, e304-318; quiz e319-321, doi:10.1331/JAPhA.2014.14537 (2014); Song, K. H. *et al.* alpha-Lipoic acid prevents diabetes mellitus in diabetes-prone obese rats. *Biochemical and biophysical research communications* **326**, 197-202, doi:10.1016/j.bbrc.2004.10.213 (2005)), neuropathy (Roman-Pintos, L. M., Villegas-Rivera, G., Rodriguez-Carrizalez, A. D., Miranda-Diaz, A. G. & Cardona-Munoz, E.

G. Diabetic Polyneuropathy in Type 2 Diabetes Mellitus: Inflammation, Oxidative Stress, and Mitochondrial Function. *Journal of diabetes research* **2016**, 3425617, doi:10.1155/2016/3425617 (2016); Ziegler, D. *et al.* Treatment of symptomatic diabetic peripheral neuropathy with the anti-oxidant alpha-lipoic acid. A 3-week multicentre randomized controlled trial (ALADIN Study). *Diabetologia* **38**, 1425-1433 (1995)), obesity (Namazi, N., Larijani, B. & Azadbakht, L. Alpha-lipoic acid supplement in obesity treatment: A systematic review and meta-analysis of clinical trials. *Clinical nutrition (Edinburgh, Scotland)* **37**, 419-428, doi:10.1016/j.clnu.2017.06.002 (2018)), non-alcoholic fatty liver disease (Gianturco, V. *et al.* Impact of combined therapy with alpha-lipoic and ursodeoxycolic acid on nonalcoholic fatty liver disease: double-blind, randomized clinical trial of efficacy and safety. *Hepatology international* **7**, 570-576, doi:10.1007/s12072-012-9387-y (2013); Hosseinpour-Arjmand, S., Amirkhizi, F. & Ebrahimi-Mameghani, M. The effect of alpha-lipoic acid on inflammatory markers and body composition in obese patients with non-alcoholic fatty liver disease: A randomized, double-blind, placebo-controlled trial. *Journal of clinical pharmacy and therapeutics* **44**, 258-267, doi:10.1111/jcpt.12784 (2019); Jung, T. S. *et al.* alpha-lipoic acid prevents non-alcoholic fatty liver disease in OLETF rats. *Liver international : official journal of the International Association for the Study of the Liver* **32**, 1565-1573, doi:10.1111/j.1478-3231.2012.02857.x (2012); Stankovic, M. N. *et al.* The effects of alpha-lipoic acid on liver oxidative stress and free fatty acid composition in methionine-choline deficient diet-induced NAFLD. *Journal of medicinal food* **17**, 254-261, doi:10.1089/jmf.2013.0111 (2014)), neurodegeneration (Erdogan, M. E. *et al.* The effects of lipoic acid on redox status in brain regions and systemic circulation in streptozotocin-induced sporadic Alzheimer's disease model. *Metabolic brain disease* **32**, 1017-1031, doi:10.1007/s11011-017-9983-6 (2017); Rodriguez-Perdigon, M., Solas, M., Moreno-Aliaga, M. J. & Ramirez, M. J. Lipoic acid improves neuronal insulin signalling and rescues cognitive function regulating VGlut1 expression in high-fat-fed rats: Implications for Alzheimer's disease. *Biochimica et biophysica acta* **1862**, 511-517, doi:10.1016/j.bbadis.2016.01.004 (2016); Zhao, H. *et al.* Neurochemical effects of the R form of alpha-lipoic acid and its neuroprotective mechanism in cellular models of Parkinson's disease. *The international journal of biochemistry & cell biology* **87**, 86-94, doi:10.1016/j.biocel.2017.04.002 (2017); Zhou, B. *et al.* Alpha Lipoamide Ameliorates Motor Deficits and Mitochondrial Dynamics in the Parkinson's Disease Model Induced by 6-Hydroxydopamine. *Neurotoxicity research* **33**, 759-767, doi:10.1007/s12640-017-9819-5 (2018)), and other vascular diseases Ozgun, E. *et al.* The effect of lipoic acid in the prevention of myocardial infarction in diabetic rats. *Bratislavske*

lekarske listy **119**, 664-669, doi:10.4149/bll_2018_119 (2018); Scaramuzza, A. *et al.* Alpha-Lipoic Acid and Antioxidant Diet Help to Improve Endothelial Dysfunction in Adolescents with Type 1 Diabetes: A Pilot Trial. *Journal of diabetes research* **2015**, 474561, doi:10.1155/2015/474561 (2015); Tromba, L., Perla, F. M., Carbotta, G., Chiesa, C. & Pacifico, L. Effect of Alpha-Lipoic Acid Supplementation on Endothelial Function and Cardiovascular Risk Factors in Overweight/Obese Youths: A Double-Blind, Placebo-Controlled Randomized Trial. *Nutrients* **11**, doi:10.3390/nu11020375 (2019); Zhao, L. & Hu, F. X. alpha-Lipoic acid treatment of aged type 2 diabetes mellitus complicated with acute cerebral infarction. *European review for medical and pharmacological sciences* **18**, 3715-3719 (2014)). The therapeutic use of ALA in improving insulin sensitivity and promoting glucose metabolism has been well documented in both human and animal models of obesity associated with IR and T2D (Evans, J. L. & Goldfine, I. D. Alpha-lipoic acid: a multifunctional antioxidant that improves insulin sensitivity in patients with type 2 diabetes. *Diabetes technology & therapeutics* **2**, 401-413, doi:10.1089/15209150050194279 (2000); Jacob, S. *et al.* Enhancement of glucose disposal in patients with type 2 diabetes by alpha-lipoic acid. *Arzneimittel-Forschung* **45**, 872-874 (1995); Erdogan, M. E. *et al.* The effects of lipoic acid on redox status in brain regions and systemic circulation in streptozotocin-induced sporadic Alzheimer's disease model. *Metabolic brain disease* **32**, 1017-1031, doi:10.1007/s11011-017-9983-6 (2017); Bitar, M. S., Wahid, S., Pilcher, C. W., Al-Saleh, E. & Al-Mulla, F. Alpha-lipoic acid mitigates insulin resistance in Goto-Kakizaki rats. *Hormone and metabolic research = Hormon- und Stoffwechselforschung = Hormones et metabolisme* **36**, 542-549, doi:10.1055/s-2004-825760 (2004); Genazzani, A. D. *et al.* Modulatory effects of alpha-lipoic acid (ALA) administration on insulin sensitivity in obese PCOS patients. *Journal of endocrinological investigation* **41**, 583-590, doi:10.1007/s40618-017-0782-z (2018); Gupte, A. A., Bomhoff, G. L., Morris, J. K., Gorres, B. K. & Geiger, P. C. Lipoic acid increases heat shock protein expression and inhibits stress kinase activation to improve insulin signaling in skeletal muscle from high-fat-fed rats. *Journal of applied physiology (Bethesda, Md. : 1985)* **106**, 1425-1434, doi:10.1152/japplphysiol.91210.2008 (2009); Henriksen, E. J. Exercise training and the antioxidant alpha-lipoic acid in the treatment of insulin resistance and type 2 diabetes. *Free radical biology & medicine* **40**, 3-12, doi:10.1016/j.freeradbiomed.2005.04.002 (2006); Henriksen, E. J. *et al.* Stimulation by alpha-lipoic acid of glucose transport activity in skeletal muscle of lean and obese Zucker rats. *Life sciences* **61**, 805-812 (1997); Kandeil, M. A., Amin, K. A., Hassanin, K. A., Ali, K. M. & Mohammed, E. T. Role of lipoic acid on insulin resistance and leptin in experimentally diabetic rats. *Journal of diabetes and its complications*

25, 31-38, doi:10.1016/j.jdiacomp.2009.09.007 (2011); Karkabounas, S. *et al.* Effects of alpha-Lipoic Acid, Carnosine, and Thiamine Supplementation in Obese Patients with Type 2 Diabetes Mellitus: A Randomized, Double-Blind Study. *Journal of medicinal food* **21**, 1197-1203, doi:10.1089/jmf.2018.0007 (2018); Sena, C. M., Cipriano, M. A., Botelho, M. F. & Seica, R. M. Lipoic Acid Prevents High-Fat Diet-Induced Hepatic Steatosis in Goto Kakizaki Rats by Reducing Oxidative Stress Through Nrf2 Activation. *International journal of molecular sciences* **19**, doi:10.3390/ijms19092706 (2018)). Interestingly, administration of ALA inhibited JNK and IKKβ activation, reduced the phosphorylation of IRS1 at the inactivating serine 307 residue, enhanced the PI3K/AKT pathway and consequently, stimulated both basal and insulin-mediated translocation of glucose transporters to the plasma membrane (Gupte, A. A., Bomhoff, G. L., Morris, J. K., Gorres, B. K. & Geiger, P. C. Lipoic acid increases heat shock protein expression and inhibits stress kinase activation to improve insulin signaling in skeletal muscle from high-fat-fed rats. *Journal of applied physiology (Bethesda, Md.: 1985)* **106**, 1425-1434, doi:10.1152/japplphysiol.91210.2008 (2009); Henriksen, E. J. *et al.* Stimulation by alpha-lipoic acid of glucose transport activity in skeletal muscle of lean and obese Zucker rats. *Life sciences* **61**, 805-812 (1997); Estrada, D. E. *et al.* Stimulation of glucose uptake by the natural coenzyme alpha-lipoic acid/thioctic acid: participation of elements of the insulin signaling pathway. *Diabetes* **45**, 1798-1804 (1996); Konrad, D. *et al.* The antihyperglycemic drug alpha-lipoic acid stimulates glucose uptake via both GLUT4 translocation and GLUT4 activation: potential role of p38 mitogen-activated protein kinase in GLUT4 activation. *Diabetes* **50**, 1464-1471 (2001); Kouzi, S. A., Yang, S., Nuzum, D. S. & Dirks-Naylor, A. J. Natural supplements for improving insulin sensitivity and glucose uptake in skeletal muscle. *Frontiers in bioscience (Elite edition)* **7**, 94-106 (2015); Qin, Z. Y. *et al.* alpha-Lipoic acid ameliorates impaired glucose uptake in LYRM1 overexpressing 3T3-L1 adipocytes through the IRS-1/Akt signaling pathway. *Journal of bioenergetics and biomembranes* **44**, 579-586, doi:10.1007/s10863-012-9460-1 (2012); Vinayagamoorthi, R., Bobby, Z. & Sridhar, M. G. Antioxidants preserve redox balance and inhibit c-Jun-N-terminal kinase pathway while improving insulin signaling in fat-fed rats: evidence for the role of oxidative stress on IRS-1 serine phosphorylation and insulin resistance. *The Journal of endocrinology* **197**, 287-296, doi:10.1677/joe-08-0061 (2008); Wang, Y. M. *et al.* alpha-Lipoic acid protects 3T3-L1 adipocytes from NYGGF4 (PID1) overexpression-induced insulin resistance through increasing phosphorylation of IRS-1 and Akt. *Journal of bioenergetics and biomembranes* **44**, 357-363, doi:10.1007/s10863-012-9440-5 (2012); Yang, Y. *et al.* Alpha-

lipoic acid attenuates insulin resistance and improves glucose metabolism in high fat diet-fed mice. *Acta pharmacologica Sinica* **35**, 1285-1292, doi:10.1038/aps.2014.64 (2014); Yaworsky, K., Somwar, R., Ramlal, T., Tritschler, H. J. & Klip, A. Engagement of the insulin-sensitive pathway in the stimulation of glucose transport by alpha-lipoic acid in 3T3-L1 adipocytes. *Diabetologia* **43**, 294-303 (2000)).

[0010] The underlying molecular mechanisms by which ALA mediates those beneficial effects are not yet fully elucidated, but the implication of several components of the HSR has been documented (Gupte, A. A., Bomhoff, G. L., Morris, J. K., Gorres, B. K. & Geiger, P. C. Lipoic acid increases heat shock protein expression and inhibits stress kinase activation to improve insulin signaling in skeletal muscle from high-fat-fed rats. *Journal of applied physiology (Bethesda, Md. : 1985)* **106**, 1425-1434, doi:10.1152/japplphysiol.91210.2008 (2009); McCarty, M. F. Versatile cytoprotective activity of lipoic acid may reflect its ability to activate signalling intermediates that trigger the heat-shock and phase II responses. *Medical hypotheses* **57**, 313-317, doi:10.1054/mehy.2001.1320 (2001); Mirjana, M. *et al.* Alpha-lipoic acid preserves the structural and functional integrity of red blood cells by adjusting the redox disturbance and decreasing O-GlcNAc modifications of antioxidant enzymes and heat shock proteins in diabetic rats. *European journal of nutrition* **51**, 975-986, doi:10.1007/s00394-011-0275-3 (2012); Oksala, N. K. *et al.* Heat shock protein 60 response to exercise in diabetes: effects of alpha-lipoic acid supplementation. *Journal of diabetes and its complications* **20**, 257-261, doi:10.1016/j.jdiacomp.2005.07.008 (2006); Oksala, N. K. *et al.* Alpha-lipoic Acid modulates heat shock factor-1 expression in streptozotocin-induced diabetic rat kidney. *Antioxidants & redox signaling* **9**, 497-506, doi:10.1089/ars.2006.1450 (2007); Strokov, I. A. *et al.* The function of endogenous protective systems in patients with insulin-dependent diabetes mellitus and polyneuropathy: effect of antioxidant therapy. *Bulletin of experimental biology and medicine* **130**, 986-990 (2000)). Recent data from our laboratory demonstrated the impaired expression of DNAJB3; a member of DNAJ/HSP40 cochaperone family in obese (Abubaker, J. *et al.* DNAJB3/HSP-40 cochaperone is downregulated in obese humans and is restored by physical exercise. *PloS one* **8**, e69217, doi:10.1371/journal.pone.0069217 (2013); Tiss, A. *et al.* Immunohistochemical profiling of the heat shock response in obese non-diabetic subjects revealed impaired expression of heat shock proteins in the adipose tissue. *Lipids in health and disease* **13**, 106, doi:10.1186/1476-511x-13-106 (2014)), and in T2D patients (Abu-Farha, M. *et al.* DNAJB3/HSP-40 cochaperone improves insulin signaling and enhances glucose uptake in vitro through JNK repression. *Scientific reports* **5**, 14448,

doi:10.1038/srep14448 (2015)), and that low levels of DNAJB3 were associated with enhanced metabolic stress50. We further demonstrated the positive effect of a 3-month physical exercise in restoring the normal expression of DNAJB3 with the concomitant improvement of various physical, biochemical and clinical parameters, suggesting thus a protective role of DNAJB3 against metabolic diseases associated with increased IR (Abubaker, J. *et al.* DNAJB3/HSP-40 cochaperone is downregulated in obese humans and is restored by physical exercise. *PloS one* **8**, e69217, doi:10.1371/journal.pone.0069217 (2013)). More recently, we provided evidence for a novel role of DNAJB3 in attenuating various forms of metabolic stress as well as in promoting insulin action and glucose uptake in 3T3-L1 adipocytes and C2C12 skeletal muscle cells (Abu-Farha, M. *et al.* DNAJB3/HSP-40 cochaperone improves insulin signaling and enhances glucose uptake in vitro through JNK repression. *Scientific reports* **5**, 14448, doi:10.1038/srep14448 (2015); Arredouani, A. *et al.* DNAJB3 attenuates metabolic stress and promotes glucose uptake by eliciting Glut4 translocation. *Scientific reports* **9**, 4772, doi:10.1038/s41598-019-41244-8 (2019)). Given the similarities in metabolic actions elicited by DNAJB3 overexpression and ALA treatment, we hypothesized that DNAJB3 might represent a molecular intermediate through which ALA mediates its beneficial actions.

SUMMARY

[0011] In a general embodiment, the present disclosure provides compositions and methods for diagnosing, prevention and/or treatment for conditions linked to insulin resistance (IR).

[0012] In some embodiments, the present disclosure provides a biomarker for diagnosis of a chronic condition linked to IR, the biomarker comprising a polypeptide encoded by DNAJB3, wherein the chronic condition is selected from the group consisting of diabetes, metabolic syndrome and their complications. Overexpression of the DNAJB3 enhances basal and insulin-stimulated glucose uptake. Overexpression of DNAJB3 elicits Glut4 translocation to the plasma membrane in C2C12 cells. Overexpression of DNAJB3 alleviates basal ER stress and enhances the oxidative stress scavenging system. DNAJB3 abrogated both JNK1 and IKKβ pathways. DNAJB3 suppressed TNF-α-mediated IL-6 promoter activation and mRNA expression.

[0013] In some embodiments, the present disclosure provides a method comprising using a biomarker comprising a polypeptide encoded by DNAJB3 to diagnose a chronic condition linked to IR, wherein the chronic condition is selected from the group consisting of diabetes, metabolic syndrome and their complications. The biomarker is used as an early molecular

signature to detect early cellular, molecular and biochemical aberrations underpinning IR and diabetes.

[0014] In some embodiments, the present disclosure provides a pharmaceutical compound comprising ALA, wherein the pharmaceutical composition is configured to prevent and/or treat a chronic condition linked to IR, and the chronic condition is selected from the group consisting of diabetes, metabolic syndrome and their complications.

[0015] In some embodiments, the present disclosure provides a method for preventing and/or treating a chronic condition linked to IR in a subject in need of same, the method comprising administering a compound comprising ALA to the subject, wherein the chronic condition is selected from the group consisting of diabetes, metabolic syndrome and their complications. The ALA is used to induce the endogenous expression of DNAJB3 gene/protein or recapitulate the activity of DNAJB3. C2C12 cells are pre-treated with the ALA to alleviate tunicamycin-induced ER stress. The ALA is used to stimulate the expression of mitochondrial markers and the oxidative stress scavenging system in C2C12 cells.

BRIEF DESCRIPTION OF DRAWINGS

[0016] Features and advantages of the invention described herein may be better understood by reference to the accompanying figures in which:

[0017] Fig. 1A shows the effect of overexpression of DNAJB3 in HEK-293 cells on preventing the phosphorylation of JNK (P-JNK) in response to phorbol myristate acetate (PMA) as compared to pCMV and pCMV-HDAC4. Full-length blots are displayed in Fig. 8.

[0018] Fig. 1B shows the effect of overexpression of DNAJB3 in HEK-293 cells on abrogating PMA-mediated AP-1-dependent transactivation in luciferase assays.

[0019] Fig. 2A shows the effect of overexpression of DNAJB3 in C2C12 cells on preventing the activation of κB-dependent transactivation in response to PMA in luciferase assays.

[0020] Fig. 2B shows the effect of overexpression of DNAJB3 in C2C12 cells on abrogating TNF-α-mediated both κB- and IL-6 promoter-dependent luciferase activation.

[0021] Fig. 3A shows the effect of overexpression of DNAJB3 on reducing the endogenous expression of IL-16 mRNA in response to TNF-α in C2C12.

[0022] Fig. 3B shows the effect of overexpression of DNAJB3 on reducing the endogenous expression of IL-16 mRNA in response to TNF-α in 3T3-L1 adipocytes.

[0023] Fig. 3C shows that silencing the expression of DNAJB3 in C2C12 myoblast with specific siRNA reduced significantly the expression of DNAJB3 mRNA in a dose dependent-manner. GAPDH gene was used as a reference for normalization.

[0024] Fig. 3D shows that knocking down the expression of DNAJB3 in C2C12 myoblasts with specific siRNA resulted in a significant increase in TNF-α-mediated IL-6 mRNA expression.

[0025] Fig. 3E shows the effect of overexpression of DNAJB3 in C2C12 myoblasts on reducing the translocation of p65 NF-κB to the nucleus in response to LPS treatment (1 μg/ml for 3 h). Full-length blots are displayed in Fig. 9.

[0026] Fig. 4A shows the effect of overexpression of DNAJB3 on preventing Tunicamycin – mediated ATF6 activation in C2C12 cells using a luciferase assay.

[0027] Fig. 4B shows the effect of overexpression of DNAJB3 on abrogating Tunicamycin-mediated mRNA expression of XBP-1 in C2C12 cells.

[0028] Fig. 4C shows the effect of overexpression of DNAJB3 on abrogating Tunicamycin-mediated mRNA expression of GRP78 in C2C12 .

[0029] Fig. 4D shows the effect of overexpression of DNAJB3 in C2C12 cells on stimulating the endogenous mRNA expression of Catalase and Glutathione peroxidase 1 (GPX1) genes in response to 300 μM H2O2 treatment for 3 h.

[0030] Fig. 5A shows dose response effect of insulin on glucose uptake in myoblasts (dashed box) and myotubes (black box).

[0031] Fig. 5B shows the expression pattern of DNAJB3 in myoblasts and myotubes as monitored by RT-PCR..

[0032] Fig. 5C shows the expression pattern of DNAJB3 in myoblasts and myotubes as monitored by Western blot.

[0033] Fig. 5D shows the effect of DNAJB3 overexpression on promoting both basal and insulin-stimulated glucose uptake in myoblasts as compared to pCMV.

[0034] Fig. 5E shows the effect of DNAJB3 overexpression on promoting glucose uptake in 3T3-L1 adipocytes.

[0035] Fig. 5F shows the effect DNAJB3 overexpression on promoting glucose uptake in HepG2 cells.

[0036] Fig. 5G shows that silencing the expression of DNAJB3 with 10 nM of specific siRNA blunted the expression of DNAJB3 mRNA in C2C12 myoblasts.

[0037] Fig. 5H shows that knocking down the expression of DNAJB3 expression with specific siRNA abrogated both basal and insulin-stimulated glucose uptake in C2C12 cells.

[0038] Fig. 6A shows the effect of DNAJB3 overexpression on the endogenous expression of Glut1 and Glut4 mRNA in C2C12 cells.

[0039] Fig. 6B shows effect of DNAJB3 overexpression on Glut4 protein expression in C2C12 cells. Full-length blots are displayed in Fig. 10.

[0040] Fig. 6C is a schematic representation of HA-Glut4-GFP construct showing the exofacial HA epitope and the GFP tag at the C-terminal region.

[0041] Fig. 6D shows representative confocal microscopy images showing cell surface staining of tagged GLUT4 in response to stimulation with 100 nM of insulin in C2C12 cells.

[0042] Fig. 6E shows the cellular localization of HA-Glut4-GFP in cells transfected with pCMV and DNAJB3 at baseline (a,b and c versus g,h and i) and after stimulation with 100 nM of insulin (d,e and f versus j,k and l).

[0043] Fig. 6F shows representative image illustrating the plasma membrane localization of HA-Glut4-GFP in C2C12 cotransfected DNAJB3 in the presence of insulin.

[0044] Fig. 6G shows the surface-to-total Glut4 ratio (HA/GFP) at baseline and after insulin simulation was determined by quantitative immunofluorescence and presented as percent change.

[0045] Figs. 7A and 7B are schematic representation for the role of DNAJB3 in mitigating metabolic stress and improving glucose uptake.

[0046] Fig. 8 shows the full-length western blots of Fig. 1A.

[0047] Fig. 9 shows the full-length western blots of Fig. 3E.

[0048] Fig. 10 shows the full-length western blots of Fig. 6B.

[0049] Fig. 11A shows RT-PCR data showing the effect of 0.3 mM ALA for 24h on the expression of representative components of the heat shock response in C2C12 cells.

[0050] Fig. 11B shows dose response effect of ALA on the expression of DNAJB3 mRNA in C2C12 cells. Full-length blots are displayed in Fig. 16.

[0051] Fig. 11C shows dose response effect of ALA on the expression of DNAJB3 protein in C2C12 cells. Full-length blots are displayed in Fig. 16

[0052] Fig. 11D shows ALA at 0.3 mM for 24h also increases the expression of DNAJB3 mRNA in HepG2 cells.

[0053] Fig. 11E shows heat shock treatment induces the expression of DNAJB3 mRNA in C2C12 cells.

[0054] Fig. 12A shows pre-treatment of C2C12 cells with 0.3 mM ALA abolishes significantly the mRNA expression of classical ER stress markers in response to tunicamycin stimulation.

[0055] Fig. 12B shows pre-treatment of C2C12 cells with 0.3 mM ALA abolishes significantly the mRNA expression of classical ER stress markers in response to tunicamycon/glucolipotoxicity stimulation.

[0056] Fig. 12C shows western blot confirming the effect of ALA on tunicamycin-induced expression of GRP78 protein in C2C12 cells. Full-length blots are displayed in Fig. 17.

[0057] Fig. 12D shows ALA reduces ATF6-dependent luciferase activity in response to tunicamycin using a functional luciferase-based assay in C2C12 cells.

[0058] Fig. 12E shows ALA reduces ATF6-dependent luciferase activity in response to tunicamycin using a functional luciferase-based assay in HepG2 cells.

[0059] Fig. 13A shows ALA treatment triggers a significant increase in the expression involved in mitochondrial biogenesis and function.

[0060] Fig. 13B shows ALA stimulates the endogenous mRNA expression of Catalase, Superoxide dismutase 1 (SOD1) and Glutathione peroxidase 1 (GPX1) genes in response to 300 μM H2O2 treatment for 3 h.

[0061] Fig. 14A shows knocking down the expression of DNAJB3 expression with 20 nM of specific siRNA blunted the endogenous expression of DNAJB3 in C2C12 cells. Actin gene was used as a reference control.

[0062] Fig. 14B shows ALA fails to protect cells from tunicamycin-induced mRNA expression of ER stress markers in C2C12 cells transfected with siRNA specific for DNAJB3.

[0063] Fig. 14C shows ALA fails to protect cells from tunicamycin-induced ATF6-dependent luciferase activity in C2C12 cells transfected with siRNA specific for DNAJB3.

[0064] Fig. 15A shows effect of ALA on insulin-stimulated glucose uptake in C2C12 cells.

[0065] Fig. 15B shows silencing the expression of DNAJB3 abrogated the effect of ALA on insulin-stimulated glucose uptake as compared to scrambled siRNA control in C2C12 cells.

[0066] Fig. 16 shows the full-length western blots of Figs. 11B and 11C.

[0067] Fig. 17 shows the full-length western blots of Fig. 12C.

[0068] Fig. 18A shows the nucleotide sequence of the human DNAJB3 cDNA.

[0069] Fig. 18B shows the protein sequence of the human DNAJB3.

[0070] Fig. 18C is the Schematic representation of the NF-KB-dependent reporter plasmids used in Luciferase assays.

DETAILED DESCRIPTION

[0071] All numerical ranges herein should be understood to include all integers, whole or fractions, within the range. Moreover, these numerical ranges should be construed as providing support for a claim directed to any number or subset of numbers in that range. For example, a disclosure of from 1 to 10 should be construed as supporting a range of from 1 to 8, from 3 to 7, from 1 to 9, from 3.6 to 4.6, from 3.5 to 9.9, and so forth.

[0072] As used herein and in the appended claims, the singular form of a word includes the plural, unless the context clearly dictates otherwise. Thus, the references "a," "an" and "the" are generally inclusive of the plurals of the respective terms. For example, reference to "an ingredient" or "a method" includes a plurality of such "ingredients" or "methods." The term "and/or" used in the context of "X and/or Y" should be interpreted as "X," or "Y," or "X and Y."

[0073] Similarly, the words "comprise," "comprises," and "comprising" are to be interpreted inclusively rather than exclusively. Likewise, the terms "include," "including" and "or" should all be construed to be inclusive, unless such a construction is clearly prohibited from the context. However, the embodiments provided by the present disclosure may lack any element that is not specifically disclosed herein. Thus, a disclosure of an embodiment defined using the term "comprising" is also a disclosure of embodiments "consisting essentially of' and "consisting of' the disclosed components. Where used herein, the term "example," particularly when followed by a listing of terms, is merely exemplary and illustrative, and should not be deemed to be exclusive or comprehensive. Any embodiment disclosed herein can be combined with any other embodiment disclosed herein unless explicitly indicated otherwise.

[0074] The term "patient" is understood to include an animal, especially a mammal, and more especially a human that is receiving or intended to receive treatment, as treatment is herein defined. While the terms "individual" and "patient" are often used herein to refer to a human, the present disclosure is not so limited. Accordingly, the terms "individual" and "patient" refer to any animal, mammal or human that can benefit from the treatment.

[0075] The terms "treatment" and "treating" include any effect that results in the improvement of the condition or disorder, for example lessening, reducing, modulating, or eliminating the condition or disorder. The term does not necessarily imply that a subject is treated until total recovery. Non-limiting examples of "treating" or "treatment of" a condition or disorder include: (1) inhibiting the condition or disorder, i.e. arresting the development of the condition or disorder or its clinical symptoms and (2) relieving the condition or disorder, i.e. causing the temporary or permanent regression of the condition or disorder or its clinical symptoms. A treatment can be patient- or doctor-related.

[0076] The terms "prevention" or "preventing" mean causing the clinical symptoms of the referenced condition or disorder to not develop in an individual that may be exposed or predisposed to the condition or disorder but does not yet experience or display symptoms of the condition or disorder. The terms "condition" and "disorder" mean any disease, condition, symptom, or indication.

[0077] The relative terms "improved," "increased," "enhanced" and the like refer to the effects of the methods and compositions disclosed herein.

[0078] The present disclosure provides a novel drug target/biomarker to attenuate metabolic stress and prevent and/or treat IR in insulin-responsive sites and more particularly to prevent and/or treat chronic conditions linked to IR including diabetes, metabolic syndrome and their complications. The present disclosure also provides methods of using such a novel drug target/biomarker to attenuate metabolic stress and prevent and/or treat IR in insulin-responsive sites and more particularly to prevent and/or treat chronic conditions linked to IR including diabetes, metabolic syndrome and their complications.

[0079] The inventors used a series of functional assays to investigate the in vitro role of DNAJB3 in modulating metabolic stress and improving glucose uptake in HEK-293, C2C12 and 3T3-L1 cells. Using JNK1- and IKKβ-dependent luciferase reporters, the inventors observed a significant decrease in luciferase activity by DNAJB3 in response to phorbol myristate acetate (PMA) and tumor necrosis factor-α (TNF-α). Furthermore, TNF-α-mediated IL-6 promoter activation and the endogenous mRNA expression are significantly abrogated by

DNAJB3. The inventors also found that DNAJB3 stimulates glucose uptake in C2C12 cells by eliciting Glut4 translocation to the plasma membrane. These results prove the physiological role of DNAJB3 in mitigating metabolic stress and regulating glucose homeostasis and insulin signaling, and as such, it could represent a potential therapeutic target for metabolic diseases caused by increased IR.

[0080] More specifically, the novel drug target/biomarker can include a polypeptide encoded by DNAJB3/HSP-40 with anti-inflammatory activity that acts as natural inhibitor of the inflammatory κB kinase β (IKKβ). IKKβ is a crucial enzyme involved in the pathogenesis of IR, T2D mellitus and metabolic syndrome.

[0081] The human DNAJB3 gene encodes a DNAJ (Heat shock protein 40; Hsp40) homolog, subfamily B, member 3 chaperone protein (DNAJB3), which can be down-regulated in disease conditions, as observed in decreased expression of DNAJB3 mRNA in peripheral blood mononuclear cells (PBMC) of obese patients.

[0082] The inventors surprisingly discovered the positive effects of DNAJB3 in enhancing glucose metabolism, eliciting the translocation of Glut4 transporter to the plasma membrane, and improving mitochondrial function/biogenesis.

[0083] The present disclosure further provides compositions comprising small molecules, such as ALA, for preventing and/or treating chronic conditions linked to IR including diabetes, metabolic syndrome and their complications. The present disclosure also provides methods of using such small molecules as ALA for preventing and/or treating chronic conditions linked to IR including diabetes, metabolic syndrome and their complications. The inventors surprisingly discovered that small molecules, such as ALA, can induce the endogenous expression of DNAJB3 gene/protein or recapitulate the activity of DNAJB3.

[0084] Furthermore, the present disclosure provides methods of using DNAJB3 as an early molecular signature or biomarker for diagnose the early cellular, molecular and biochemical aberrations underpinning IR and diabetes (e.g., T2D).

[0085] EXAMPLE 1

[0086] **Cell Culture.** C2C12 myoblasts, 3T3-L1 preadipocytes, HEK-293 and HepG2 cells were all obtained from ATCC and maintained in DMEM supplemented with 10% FBS and 1% penicillin/streptomycin at 37 °C and 5% CO2. Differentiation of C2C12 myoblasts to myotubes was done by replacing FBS with 2% horse serum with a daily change of the media for 7 days. 3T3-L1 were differentiated from preadipocytes to adipocytes using isobutylmethylxanthine

(IBMX), dexamethasone and insulin as we previously described. All the cells were used before the 25th passage.

[0087] **Plasmids and silencing RNA.** pCMV-DNAJB3 and pCMV-HSPA1A plasmids were purchased from Origene (Origene Technologies, Inc., Rockvile, MD). They encode the human DNAJB3 and HSP-72, respectively. pCMV6 empty vector was used as a negative control. pHA-Glut4-GFP was a gift from Dr. MacGraw (Weill Cornell University, New York, NY) and consists of an exofacial HA epitope and a GFP tag located at the N-terminal and C-terminal of Glut4, respectively. Reporter plasmids carrying firefly luciferase gene under the control of three copies of either wild type (3xwt-κB-Luc) or mutant (3xμκB-Luc) NF-κB binding site were described previously. Reporter plasmid carrying the human IL-6 promoter (pIL6-Luc651), was obtained from Dr. Eickelberg (University of Colorado Denver, Aurora, CO). Reporter plasmid carrying seven copies of AP-1 binding site upstream of the firefly luciferase gene was obtained from Dr. Fahmi (Montreal University, Montreal, QC). ATF6-dependent reporter plasmid consisting of three copies of ATF6 response element upstream of the luciferase gene was purchased from Promega (Promega Corporation, Madison, WI). In all cases, Renilla Luciferase vector under the control of CMV promoter (pRL-CMV; Promega Corporation, Madison, WI) was used as internal control. Three different siRNA molecules specific for DNAJB3 and the scrambled siRNA were used to knockdown the expression of DNAJB3 in C2C12 (#SR406762; Origene Technologies, Inc., Rockville, MD).

[0088] **Transient transfections.** Lipofectamine 3000 and RNAiMAX lipofectamine (Invitrogen, Carlsbad, CA) were used for transient DNA and siRNA transfection, respectively. All the functional assays were analyzed at least in triplicate and a minimum of three independent experiments.

[0089] **Luciferase assays.** HEK-293 and C2C12 were transfected with 5 μg of the reporter plasmid and 10 μg of either pCMV-DNAJB3 or pCMV and then, plated on 96-well plates at 1.104 cells/well followed by a 24-h incubation. Cells were then treated with 25 ng/ml of TNF-α (R&D Systems, Minneapolis, MN) or 5 μM PMA (Sigma Aldrich, St. Louis, MO) or 0.5 μg/ml Tunicamycin (Sigma Aldrich, St. Louis, MO) for 16 h and afterwards, harvested for luciferase assays using the Bright Glo Luciferase Assay kit (Promega, Madison, WI). Luciferase activity was measured either on Spark® 10 M plate reader (Tecan, Männedorf, Switzerland) or Glomax multi detection plate reader (Promega, Madison, WI). Differences in transfection efficiency were normalized with pRL-CMV internal control.

[0090] **Measurement of gene expression by real-time PCR (RT-PCR).** Upon 48 h transfection of C2C12 and 3T3-L1 cells with 7.5 μg of either pCMV-DNAJB3 or pCMV and stimulation with either the vehicle, 3 h incubation with 50 ng/ml TNF-α (R&D Systems, Minneapolis, MN) or an overnight incubation with 0.5μg/ml Tunicamycin (Sigma Aldrich, St. Louis, MO), total RNA was extracted using RNeasy Plus Universal Mini Kit (Qiagen, Hilden, Germany). It was then converted to cDNA using MMLV Reverse Transcriptase Kit (Invitrogen, Carlsband, CA) and analyzed by RT-PCR on QuantStudio 6 Flex system (ThermoFisher, Waltham, MA), using SYBR Green. Relative expression was calculated by the comparative ΔΔCT method. The sequences of the primers used in this study are listed in Table 1.

[0091] **Table 1**

	Forward	Reverse
DNAJB3	5′-AGGGGCTGTACCCTTCTCTA-3	5′-AGTTTCCTGGAGAACCGAAG-3′
IL-6	5′-GATGGATGCTACCAAACTGG-3′	5′-TGAAGGACTCTGGCTTTGTC-3′
Glut4	5′-TGGGTCCTTACGTCTTCCTT-3′	5′-GCTGAGATCTGGTCAAACGT-3′
Glut1	5′-TACCAAAGTTATCCGGCAGC-3′	5′-CTCTGAGTCTCAATGGCCAC-3′
Actin	5′-AAGAGCTATGAGCTGCCTGA-3′	5′- GATGCCACAGGATTCCATAC-3′
GAPDH	5′-CTGGAGAAACCTGCCAAGTA-3′	5′-AGTGGGAGTTGCTGTTGAAG-3′
SOD1	5′-GAGAGGCATGTTGGAGACCT-3′	5′-CCACCTTTGCCCAAGTCATC-3′
Catalase	5′-AGGAGGCAGAAACTTTCCCA-3′	5′-GGCCCTGAAGCATTTTGTCA-3′
GPX1	5′-ATCAGTTCGGACACCAGGAG-3′	5′-GATGTACTTGGGGTCGGTCA-3′
XBP1	5′-TCCCCAGAACATCTTCCCAT-3′	5′-ACATGACAGGGTCCAACTTG-3′
GRP78	5′-AATTTCTGCCATGGTTCTCA-3′	5′-AGCATCTTTGGTTGCTTGTC-3′

[0092] **Preparation of the whole protein extracts, nuclear and cytoplasmic extracts.** Whole protein extracts were prepared from C2C12 and HEK-293 cells by resuspending cells in RIPA buffer (50 mM Tris-HCl pH 7.5, 150 mM NaCl, 1% Triton X-100, 0.5% Na-Deoxycholate, 0.1% SDS and Protease Inhibitor Cocktail (Sigma Aldrich, St. Louis, MO) and incubating the homogenates for 30 min at 4 °C. The extracts were then centrifuged at 13,000 rpm for 20 min and the supernatants were collected. The preparation of nuclear and cytoplasmic extracts from C2C12 myoblasts was carried out by using the ReadyPrep™ Cytoplasmic/Nuclear Extraction Kit (Bio-Rad, Hercules, CA) according to the manufacturer's

protocol. Protein concentration was determined by Bradford assay (Biorad) at 595 nm using γ-Globulin (Bio-Rad, Hercules, CA) as standard. Proteins were aliquoted and stored at −80 °C until assayed.

[0093] **Western blot analysis**. Whole protein extracts prepared from HEK-293 cells transfected with 10 μg of either pCMV-DNAJB3, pCMV or pCMV-HDAC4 vectors were used to monitor the changes in the phosphorylation levels of JNK (P-JNK) in response to 5 μM PMA stimulation by western blot essentially as we described previously (Zhao, H. *et al.* Neurochemical effects of the R form of alpha-lipoic acid and its neuroprotective mechanism in cellular models of Parkinson's disease. *The international journal of biochemistry & cell biology* **87**, 86-94, doi:10.1016/j.biocel.2017.04.002 (2017)). The expression of DNAJB3 and HSP-72 in whole cell extracts prepared from myoblasts and myotubes was also performed by western blot using anti-DNAJB3 (Proteintech Group, Inc., Chicago, IL) and anti-HSP-72 (ENZO Life Sciences, Inc., Farmingdale, NY) antibodies. The endogenous expression of Glut4 in C2C12 overexpressing DNAJB3 (or control vector) was monitored by western bot using anti-Glut4 antibody (Abcam, Cambridge, UK). Nuclear translocation of p65 NF-κB in C2C12 transfected with DNAJB3 or pCMV after LPS/TNF-α stimulation was carried out on cytoplasmic and nuclear fractions by western blot using anti-p65 antibody (Cell Signaling Technology, Inc., Danvers, MA). Anti-GRP78 antibody (Cell Signaling Technology, Inc., Danvers, MA) was used to monitor the expression of GRP78 protein in response to Tunicamycin treatment using whole cell extracts from C2C12 transfected with DNAJB3 or pCMV. GAPDH, β-Actin (Cell Signaling Technology, Inc., Danvers, MA) and γ-Tubulin (Acam, Cambridge, UK) were used as internal controls as indicated in the figure legends.

[0094] **Glucose uptake assay.** Cells were grown in 100 mm petri dishes until they reached 80% confluence and then, transfected with 7.5 μg of either pCMV-DNAJB3 or pCMV or 10 nM of DNAJB3-siRNA. The next day, they were plated on 96-well plates at 1.10^4 cells/well and then used to monitor glucose uptake using the fluorescent D-glucose analog (2-NBDG) (Cayman, Ann Arbor, MI) as we described previously, except that cells were glucose-starved for overnight while HepG2 cells were starved only for 3 h. After washes, the retained fluorescence was measured respectively at excitation and emission wavelengths of 485 nm and 535 nm with FLUOstar Omega microplate reader (BMG Labtech, Ortenberg, Germany).

[0095] **Monitoring Glut4 translocation by immunofluorescence and confocal microscopy.** C2C12 transfected with 5 μg of pHA-Glut4-GFP plasmid and 10 μg of either pCMV-DNAJB3 or pCMV were plated on glass-bottom dishes. After stimulation with 100 nM of Insulin (Sigma

Aldrich, St. Louis, MO), they were fixed with 4% paraformaldehyde without permeabilization and subjected to HA staining using a rabbit monoclonal anti-HA antibody (Rockland, Limerick, PA) followed by Alexa Fluor 594-conjugated goat anti-rabbit IgG (Abcam, Cambridge, UK). The Alexa Fluor 595/GFP ratio was determined by quantitative fluorescence microscopy as described previously. To avoid cell selection bias fields, cells expressing the HA–Glut4-eGFP were randomly chosen in the GFP channel blinded to the expression of HA–Glut4-GFP on the plasma membrane (Alexa Fluor 594 channel). Images were collected in both GFP and Alexa Fluor 594 channels. To optimize the dynamic range of the assay, exposure times for the channels were independently set to maximize the signal while minimizing the number of cells with expression levels above saturation. Once set for each channel, all images in that channel were collected at the same exposure. The fluorescence intensities of GFP and Alexa 594 were quantified at the single-cell level. Mock- transfected cells were used in parallel to correct for fluorescence resulting from non-specific binding of the primary and/or secondary antibodies.

[0096] **Statistical analysis.** Results are presented as means ± SEM and were plotted using GraphPad (Prism v7, La Jolla, CA). We used one-way ANOVA for comparison of the groups with post-hoc Tukey's test or the Student test, as appropriate. A P-value < 0.05 was considered statistically significant.

[0097] **Overexpression of DNAJB3 reduces JNK1 phosphorylation and abolishes its activity in a JNK1-dependent luciferase assay.** The inventors found that JNK is part of a multicomponent complex that interacts with DNAJB3 in immunoprecipitation assays (Abubaker, et al., PloS one 2013; 8: e69217).

[0098] Fig. 1A shows that DNAJB3 acts as natural inhibitor of JNK1 stress kinase. Transient overexpression of DNAJB3 in HEK-293 cells prevents the phosphorylation of JNK (P-JNK) in response to phorbol myristate acetate (PMA) as compared to pCMV and pCMV-HDAC4. Total JNK and GAPDH were used as internal controls to monitor for protein loading differences. After determining the levels of P-JNK, the same membrane was stripped and probed with antibody against total JNK antibody. Full-length blots are displayed in Fig. 8.

[0099] These results show a clear reduction in the levels of P-JNK1 in cells overexpressing DNAJB3 in response to PMA stimulation. Since JNK is also known to modulate gene expression via AP-1 cis-regulatory element (Derijard, et al., Cell 1994; 76: 1025-1037), we investigated the impact of DNAJB3 on JNK activity using a functional assay. To this end,

HEK-293 cells were co-transfected with p7xAP-1-Luc with either pCMV-DNAJB3 expression vector or pCMV vector and the luciferase activity was monitored after PMA treatment.

[00100] Fig. 1B shows that DNAJB3 abrogates PMA-mediated AP-1-dependent transactivation in luciferase assays. DMSO was used at 0.25% as a vehicle. (**$P < 0.01$; NS: Not significant.) This data indicates that PMA treatment triggers 4–5 fold increase in luciferase activity as compared to the vehicle. In cells overexpressing DNAJB3, the luciferase activity was significantly reduced ($P < 0.001$), confirming thus the observed reduced levels in P-JNK triggered by DNAJB3.

[00101] **DNAJB3 abrogates PMA and TNF-α-mediated IKKβ activation.** IKKβ has also been shown to interact with DNAJB3, however, the functional consequence of such interaction was not explored. The inventors interrogated whether DNAJB3 could interfere with NF-κB activation using our previously established κb-dependent luciferase system. To this end, cells were co-transfected with p3xwtκB-Luc reporter and either pCMV-DNAJB3 or the pCMV and subsequently, they were stimulated with 5 μM of PMA or 25 nM TNF-α and then, the luciferase activity was monitored.

[00102] Fig. 2A shows transient overexpression of DNAJB3 in C2C12 cells prevents the activation of κB-dependent transactivation in response to phorbol myristate acetate (PMA) in luciferase assays. As shown in Fig. 2A, there was a 5-fold increase of luciferase activity in response to PMA treatment in cells cotransfected with pCMV. In cells overexpressing DNAJB3, the luciferase activity was markedly reduced ($P < 0.01$; Fig. 2A).

[00103] Fig. 2B shows that DNAJB3 abrogates also TNF-α-mediated both κB- and IL-6 promoter-dependent luciferase activation. DMSO at 0.25% and PBS were used as vehicles for PMA and TNF-α treatments, respectively. A similar increase in luciferase activity following stimulation with TNF-α in cells transfected with p3xwtκB-Luc construct but not with p3xmutκB-Luc construct ($P < 0.01$; Fig. 2B). DNAJB3 overexpression abolished the κB-dependent luciferase activity triggered by TNF-α- ($P < 0.001$; Fig. 2B). The inventor then assessed the effect of DNAJB3 in controlling NF-κB activity using a physiologically relevant context such as the IL-6 promoter whose activity is in part, regulated by NF-κB. DNAJB3 reduced significantly the activity of IL-6 promoter following TNF-α stimulation ($P < 0.001$; Fig. 2B).

[00104] Together, these data indicate that DNAJB3 acts upstream of the NF-κB signaling pathway and that IKKβ is an interacting partner of DNAJB3.

[00105] **DNAJB3 modulate the expression of the IL-6 mRNA in response to TNF-α.** The inventors also investigated the effect of DNAJB3 on the endogenous expression of IL-6 mRNA by RT-PCR.

[00106] Figs. 3A-3E show that DNAJB3 is involved in TNF-α-mediated IL-6 mRNA expression. Figs. 3A and 3B show overexpression of DNAJB3 reduces significantly the endogenous expression of IL-16 mRNA in response to TNF-α both in C2C12 (Fig. 3A) and 3T3-L1 adipocytes (Fig. 3B). Fig. 3C shows silencing the expression of DNAJB3 in C2C12 myoblast with specific siRNA reduced significantly the expression of DNAJB3 mRNA in a dose dependent-manner. GAPDH gene was used as a reference for normalization. Fig. 3D shows that knocking down the expression of DNAJB3 in C2C12 myoblasts resulted in a significant increase in TNF-α-mediated IL-6 mRNA expression. Fig. 3E shows overexpression of DNAJB3 in C2C12 myoblasts reduces the translocation of p65 NF-κB to the nucleus in response to LPS treatment (1 μg/ml for 3 h). Full-length blots are displayed in Fig. 9. PBS was used as a vehicle. *$P < 0.05$; **$P < 0.01$; ***$P < 0.001$; NS: Not significant.

[00107] Results displayed in Figs. 3A and 3B show a 2- to 2.5-fold increase in IL-6 mRNA expression upon stimulation with TNF-α as compared to the vehicle ($P < 0.05$) in C2C12 and 3T3-L1 cells, respectively. Overexpression of DNAJB3 caused a significant reduction of IL-6 mRNA expression following TNF-α stimulation as compared to pCMV ($P < 0.01$) both in C2C12 myoblasts (Fig. 3A) and 3T3-L1 adipocytes (Fig. 3B). Under the same conditions, HSP-2 failed in preventing the response of IL-6 mRNA expression to TNF-α (Fig. 3A). To corroborate these findings, the inventors silenced the expression of DNAJB3 using specific siRNA. The efficiency and specificity of these siRNA to abrogate the endogenous expression of DNAJB3 were first determined by RT-PCR in C2C12 myoblasts. Transfection of cells with 10 nM DNAJB3 siRNA reduced the expression of DNAJB3 mRNA by 84% as compared to control siRNA ($P < 0.0001$; Fig. 3C). The response of IL-6 mRNA expression to TNF-α under the conditions where DNAJB3 expression is silenced was investigated in C2C12 myoblasts and the finding is displayed in Fig. 3D. As shown, there was a slight increase in both basal and TNF-α induced IL-6 mRNA expression as compared to scrambled siRNA ($P < 0.05$).

[00108] Then, the effect of DNAJB3 on the translocation of NF-κB in response to inflammatory inducers in C2C12 myoblasts was determined. Western blot was used to monitor the translocation of p65 subunit to the nucleus in response to LPS stimulation and the data are displayed in Fig. 3E. As shown, there was a decrease of approximately 60% of p65 in the nucleus in response to LPS when DNAJB3 is overexpressed as compared to pCMV. In the

cytoplasmic fraction, LPS triggered an increase in p65 levels in both pCMV and DNAJB3 transfected cells by 1.75- and 2.29-fold, respectively (Fig. 3E). These findings support further the anti-inflammatory property of DNAJB3.

[00109] **DNAJB3 has a positive effect in alleviating ER stress and enhancing the oxidative stress scavenging system.** The contribution of persistent ER stress and enhanced oxidative stress to the pathogenesis of IR and T2D promoted the inventors to assess the effect of DNAJB3 on mitigating ER stress and oxidative stress. For this purpose, the inventors used a luciferase reporter assay driven by multiple copies of ATF-6 transcription factor; the master transcription factor involved in the activation of ER stress. C2C12 myoblasts were cotransfected with ATF-6 reporter and either pCMV-DNAJB3 or pCMV and then stimulated for overnight with 0.5µg/ml of Tunicamycin.

[00110] Figs. 4A-4D show overexpression of DNAJB3 alleviates basal ER stress and enhances the oxidative stress scavenging system. Fig. 4A shows transient overexpression of DNAJB3 in C2C12 myoblasts cells reduces significantly the basal activity of ATF6 in Luciferase assays. B-C: DNAJB3 abrogates also Tunicamycin-mediated mRNA expression of both XBP-1 (Fig. 4B) and GRP78 (Fig. 4C). Fig. 4D shows overexpression of DNAJB3 in C2C12 cells stimulates the endogenous mRNA expression of Catalase and Glutathione peroxidase 1 (GPX1) genes in response to 300 µM H2O2 treatment for 3 h. DMSO at 0.25% and PBS were used as vehicles for Tunicamycin and TNF-α treatments, respectively. *$P < 0.05$; **$P < 0.01$; ***$P < 0.001$.

[00111] As shown in Fig. 4A, DNAJB3 reduces significantly ($P < 0.01$) the luciferase activity at both basal level and following Tunicamycin stimulation. This data is suggestive of a role of DNAJB3 in alleviating the ER stress. To complement this finding, we examined the effect of DNAJB3 on the endogenous expression of representative markers of ER stress; namely GRP78 and XPB1 in response to Tunicamycin. Data displayed in Figs. 4B-4C show a significant decrease in both XBP1 and GRP78 mRNA levels in DNAJB-transfected cells upon Tunicamycin treatment ($P < 0.05$).

[00112] Then the ability of DNAJB3 to modulate the expression of key representative antioxidant enzymes in response to oxidative stress was assessed. Results displayed in Fig. 4D indicate a significant increase in the expression of Catalase ($P < 0.05$) and GPX1 ($P < 0.01$) in response to H2O2 as compared to pCMV.

[00113] Taken together, these results indicate that DNAJB3 has a positive effect in reducing ER stress and enhancing the antioxidant defense system.

[00114] **DNAJB3 enhances basal and insulin-stimulated glucose uptake.** Whether overexpression of DNAJB3 in C2C12 could enhance glucose uptake as investigated. The inventors initially compared the glucose uptake in differentiated (myotubes) and undifferentiated (myoblasts) C2C12 in response to insulin and the data shown in Fig. 5A revealed a subtle difference in insulin-stimulated glucose uptake between myoblasts and myotubes.

[00115] Figs. 5A-5G show that DNAJB3 promotes glucose uptake in C2C12 cells. Fig. 5A shows that dose response effect of insulin on glucose uptake in myoblasts (dashed box) and myotubes (black box). Fig. 5B shows RT-PCR data showing the expression of DNAJB3 in myoblasts and myotubes. GAPDH was used as a control. Fig. 5C shows western blot showing the expression pattern of DNAJB3 myoblasts and myotubes. GAPDH was used as a reference for normalization. Fig. 5D shows that DNAJB3 promotes both basal and insulin-stimulated glucose uptake in myoblasts as compared to pCMV. HSP-72 has no role on glucose uptake. Figs. 5E and 5F show overexpression of DNAJB3 promotes glucose uptake in 3T3-L1 adipocytes (Fig. 5E) and HepG2 cells (Fig. 5F). Fig. 5G shows silencing the expression of DNAJB3 with 10 nM of specific siRNA blunted the expression of DNAJB3 mRNA in C2C12 myoblasts. Actin gene was used as a reference control. Fig. 5H shows knocking down the expression of DNAJB3 expression with specific siRNA abrogated both basal and insulin-stimulated glucose uptake in C2C12 cells. *$P < 0.05$; **$P < 0.01$; ***$P < 0.001$.

[00116] The expression levels of DNAJB3 mRNA and protein before and after differentiation of C2C12 cells were determined. Results displayed in Figs. 5B and 5C indicate a modest change in the levels of DNAJB3 mRNA (Fig. 5B) and protein (Fig. 5C) following differentiation of C2C12 from myoblasts to myotubes. C2C12 myoblasts was used as a surrogate cellular model to study the effect of DNAJB3 on glucose uptake in response to insulin. In transfected myoblasts, DNAJB3 triggers a significant increase in basal glucose uptake as compared to pCMV ($P < 0.05$; Fig. 5D). In response to insulin stimulation, we observed a further increase in glucose uptake in cells overexpressing DNAJB3 as compared to pCMV and HSP-72 ($P < 0.01$; Fig. 5D). In 3T3-L1 adipocytes, a significant increase was also observed in cells overexpressing DNAJB3 in response to insulin stimulation but it was less pronounced than in C2C12 cells ($P < 0.05$; Fig. 5E). The effect of DNAJB3 on glucose uptake in HepG2 cells was also investigated, and the data are displayed in Fig. 5F. As shown, DNAJB3

triggers a marked increase in basal glucose uptake in HepG2 cells as compared to pCMV ($P < 0.001$; Fig. 5F). Stimulation with insulin did not show any additive effect on glucose uptake in cells overexpressing DNAJB3 while in pCMV transfected cells, a 2-fold increase in glucose uptake was observed ($P < 0.001$; Fig. 5F). To further validate the direct role of DNAJB3 in promoting glucose uptake, the expression of DNAJB3 was silenced using siRNA. As shown in Fig. 5G, 10 nM of DNAJB3 siRNA blunted the expression of DNAJB3 mRNA in C2C12 myoblasts ($P < 0.0001$). The effect of knocking down the expression of DNAJB3 on glucose uptake was determined, and the result is displayed in Fig. 5H. As shown, knocking down the expression of DNAJB3 reduced significantly both basal ($P < 0.0001$) and insulin stimulated ($P < 0.01$) glucose uptake as compared with scrambled siRNA. These results suggest an important role of DNAJB3 in enhancing glucose uptake in various metabolically relevant cells.

[00117] **Overexpression of DNAJB3 elicits Glut4 translocation to the plasma membrane in C2C12 cells.** Glut1 and Glut4 transporters have a central role in basal and insulin-mediated glucose uptake by the skeletal muscle, respectively. To determine whether the observed increase in glucose uptake by DNAJB3 is due to increased expression of Glut transporters, we measured the expression levels of both Glut4 and Glut1 in C2C12 myoblasts transfected with either pCMV-DNAJB3 or pCMV.

[00118] Figs. 6A-6G show DNAJB3 elicits the translocation of Glut4 transporter to the plasma membrane in C2C12 cells without changing its expression. Fig. 6A shows effect of DNAJB3 on the endogenous expression of Glut1 and Glut4 mRNA. Fig. 6B shows effect of DNAJB3 on Glut4 protein expression. Full-length blots are displayed in Fig. 10. Fig. 6C shows schematic representation of HA-Glut4-GFP construct showing the exofacial HA epitope and the GFP tag at the C-terminal region. Fig. 6D shows representative confocal microscopy images showing cell surface staining of tagged GLUT4 in response to stimulation with 100 nM of insulin in C2C12 cells. Fig. 6E shows cellular localization of HA-Glut4-GFP in cells transfected with pCMV and DNAJB3 at baseline (a,b and c versus g,h and i) and after stimulation with 100 nM of insulin (d,e and f versus j,k and l). The images were captured using the tile scanning method; and each image represents 25 adjacent and overlapping fields acquired with a 40X objective. The quantification was done on individual cells and for each condition; we analyzed at least 100 cells. Fig. 6F shows representative image illustrating the plasma membrane localization of HA-Glut4-GFP in C2C12 cotransfected DNAJB3 in the presence of insulin. Fig. 6**G** shows the surface-to-total Glut4 ratio (HA/GFP) at baseline and

after insulin simulation was determined by quantitative immunofluorescence and presented as percent change. **P < 0.01.

[00119] Data displayed in Figs. 6A-6B did not reveal any change in the expression of Glut4 mRNA (Fig. 6A) and protein (Fig. 6B). By contrast, a significant increase in the levels of Glut1 mRNA was observed in cells overexpressing DNAJB3 (P < 0.001; Fig. 6A). This observation, which ruled out the direct effect of DNAJB3 on controlling the endogenous expression of Glut4 expression in C2C12 cells, prompted the inventors to investigate the effect of DNAJB3 on its translocation to the plasma membrane. Cells were transfected with pHA-Glut4-GFP (Fig. 6C) and stimulated with insulin and the cellular localization of Glut4 was visualized by confocal microscopy. As expected, the anti HA antibody labels only the Glut4 on the plasma membrane while the GFP reflect the total Glut4 expression (cell surface and intracellular) (Fig. 6D).

[00120] Cells were co-transfected with pHA-Glut4-GFP and either pCMV or DNAJB3, and Glut4 translocation was monitored by immunofluorescence. A marked increase was observed in both basal (Fig. 6E,g–i) and insulin-stimulated (Fig. 6E,j–l,F) Glut4 translocation in DNAJB3 transfected cells as compared to pCMV control both at basal level (Fig. 6E,a–c) and after insulin stimulation (Fig. 6E,d–f). Quantification of the surface-to-total Glut4 ratio (HA/GFP) revealed a 38% of the Glut4 pool is localized to plasma membrane at steady state (pCMV expression). Upon expression of DNAJB3, the surface Glut4 pool is enriched to 48% (P < 0.01; Fig. 6G). In response to insulin, the Glut4 surface pool is increased to 52% in pCMV transfected cells and to 67% in cells overexpressing DNAJB3 (P < 0.01; Fig. 6G).

[00121] Therefore, the inventors has found that DNAJB3 has a role in modulating metabolic stress and its relationship to glucose metabolism. It has been demonstrated that DNAJB3: 1- Abrogated both JNK1 and IKKβ pathways in functional assays, 2- Suppressed TNF-α-mediated IL-6 promoter activation and mRNA expression; 3- Reduced ER and oxidative stress and, 4- Enhanced glucose uptake and elicited Glut4 translocation. Altogether, the results provide for the first time a compelling evidence for a novel role of DNAJB3 in modulating metabolic stress; a prerequisite step that leads to IR and T2D.

[00122] The pathophysiological role of DNAJB3 in glucose metabolism was investigated following the inventors' observations that the levels of DNAJB3 are reduced in adipose tissue obtained from obese and diabetic subjects and they correlate with increased P-JNK1, enhanced inflammation and ER stress. More importantly, it has been shown that physical exercise training restored the normal expression of DNAJB3 while decreasing P-JNK1, inflammatory

and ER stress responses. Interestingly, the decrease in DNAJB3 levels was more pronounced in obese-diabetic patients as compared to obese non-diabetic subjects (Abu-Farha, et al., Scientific reports 2015; 5: 14448). The inventors also found that DNAJB3 interacts with JNK1 and IKKβ in co-immunoprecipitation assays (Abubaker, et al., PloS one 2013; 8: e69217) and attenuates the activation of JNK in response to palmitate (Abu-Farha, et al., Scientific reports 2015; 5: 14448).All these observations demonstrate a protective role of DNAJB3 against obesity associated metabolic stress.

[00123] One of the pathways that are activated under metabolic stress conditions is the JNK1 kinase pathway, which interferes with insulin signal transduction. The findings of the inventors indicate that beside the role of DNAJB3 in attenuating the activation of JNK1, it significantly reduces the phosphorylation of IRS-1S307 in response to palmitate while promoting the AKT survival pathway as monitored by increased phosphorylation of AKT protein in HEK-293 cells and 3T3-L1 adipocytes. In addition to its effect on IRS-1, JNK1 plays a fundamental role in modulating gene expression by activating an array of transcription factors and other nuclear proteins involved in apoptosis, inflammation, DNA repair, mRNA stability and development. The inventors found that DNAJB3 acts as a natural inhibitor of JNK-1 as it abrogates its ability to modulate gene transcription using functional assays, confirming thus the inventors' demonstration that DNAJB3 binds to JNK1 and reduces its activation in response to palmitate and PMA stressors (Figs. 1A-1B).

[00124] Besides JNK1, pathological activation of the IKKβ kinase has detrimental consequence on insulin signaling and glucose metabolism. IKKβ is also an inhibitor of IRS-1 substrate as it phosphorylates its serine 307 residue. IKKβ is a master upstream kinase that activates the canonical pathway of NF-κB. Once activated, it turns on a complex transcription program driven by NF-κB that leads to inappropriate expression and release of an array of inflammatory mediators including cytokines, chemokines, metalloproteases and growth factors. Using a κB-dependent luciferase assay, the inventors showed for the first time that both PMA- and TNF-α mediated activation of IKKβ/NF-κB axis are markedly suppressed when DNAJB3 is overexpressed (Figs. 2A-2B). To validate further the role of DNAJB3 in modulating the activity of IKKβ kinase in a biologically relevant context, cells were transfected with the luciferase reporter system driven by the entire IL-6 promoter. The inventors found a marked decrease in the transactivation of IL-6 promoter in response to TNF-α when DNAJB3 is overexpressed (Fig. 2B). These data are consistent with the immunoprecipitation data which show that DNAJB3 and IKKβ are part of a large multi-protein complex. In the setting of

obesity, the decrease in the expression of DNAJB3 was shown by the inventors to be concomitant with increased expression of IL-6 mRNA. The inventors found a functional role of DNAJB3 in reducing the endogenous expression of IL-6 mRNA both in C2C12 (Fig. 3A) and 3T3-L1 (Fig. 3B). These findings could also explain, at least in part, the paradox between DNAJB3 and IL-6 levels in obese subjects. The results showing anti-inflammatory activity of DNAJB3 are in line with the previous findings on HSP-25/27, another heat shock protein that was shown to bind to IKKβ and inhibits its activity and thereby, improving insulin signaling in skeletal muscle from high fat fed rats. HSP-72 is one of the best-studied chaperones among all the HSPs in relationship to metabolic diseases. Its role in conferring protection against metabolic defects leading to IR and T2D in part by reducing the inflammation is extensively reported. However, HSP-72 does not seem to have a role in attenuating the expression of IL-6 mRNA in C2C12 cells under our experimental conditions (Fig. 3A).

[00125] Another important aspect in this disclosure is the effect of DNAJB3 on glucose metabolism in skeletal muscle C2C12 as well as the molecular and biochemical determinants mediating such effect. Glucose transport into muscle and fat cells is an important step in insulin action and is critical for the maintenance of glucose homeostasis. The inventors have found that overexpression of DNAJB3 in 3T3-L1 adipocytes resulted in enhanced glucose uptake. The inventors have also found that DNAJB3 has a positive impact on improving insulin signaling as it prevents IRS-1S307 phosphorylation while promoting its phosphorylation at tyrosine 612 (IRS-1Y612). The inventors used two complementary approaches to investigate the specific effect of DNAJB3 on glucose uptake, namely by increasing and knocking down its expression. The inventors found that DNAJB3 enhances both basal and insulin-stimulated glucose uptake in C2C12 cells (Figs. 5A-5G). The inventors observed a significant increase in glucose uptake in cells overexpressing DNAJB3 that was independent of insulin action (Fig. 5D). An additive effect of insulin on glucose uptake was observed in C2C12 cells overexpressing DNAJB3 (Fig. 5D). In agreement with this, knocking down the expression of DNAJB3 by silencing RNA blunted the glucose uptake in response to insulin (Fig. 5H). In HepG2 however, DNAJB3 increases only the basal glucose uptake (Fig. 5F).

[00126] Finally, the inventors investigated the mechanism underlying the DNAJB3-mediated glucose uptake enhancement. In the skeletal muscle, Glut1 and Glut4 have a central role in basal and insulin-mediated glucose mobilization, respectively. The observed effect of DNAJB3 on basal glucose uptake is consistent with the finding that DNAJB3 stimulates the expression of Glut1 (Fig. 6A). Insulin elicits its metabolic action by activating multiple

signaling cascades in metabolically relevant sites. Of these, the activation of phosphatidylinositol-3-kinase (PI-3K), Akt and its substrate 160 (AS160) are critically involved in insulin-mediated Glut4 translocation and glucose uptake in 3T3-L1 adipocytes and skeletal muscle. In human subjects, Akt and AS160 phosphorylation are impaired in skeletal muscle obtained from insulin-resistant patients (Karlsson, et al., Diabetes 2005; 54: 1692-1697) as well as upon TNF-α stimulation. Surprisingly, the level P-AKT and P-AS160 were significantly increased in 3T3-L1 adipocytes overexpressing DNAJB3. The results indicate that DNAJB3 elicits both basal and insulin-stimulated Glut4 translocation in C2C12 (Figs. 6A-6G). These results provide novel insights into the regulatory mechanism by which DNAJB3 stimulates glucose uptake.

[00127] Without being bound to the theory, the inventors believe that DNAJB3 orchestrates its protective effects according to the model illustrated in Figs. 7A-7B. As indicated, excessive accumulation of free fatty acids, chronic hyperglycemia and inflammatory mediators lead to the persistent ER stress, oxidative stress and impaired expression of the HSR. This toxic environment will lead to the activation of JNK-1 and IKKβ kinases that target the IRS-1 and convert it to poor substrate of the insulin receptor and ultimately blocking the PI-3K/AKT pathway. At the nuclear level, the activation of JNK-1 and IKKβ leads to the activation of at least two transcriptional programs orchestrated by NF-κB and AP-1 transcription leading thus, to the inappropriate expression and/or release of inflammatory mediators and stress and apoptosis genes (Fig. 7A). Overexpression DNAJB3 prevents the activation of JNK-1 and IKKβ kinases and thereby favoring the PI-3K/AKT pathway that leads to Glut4 translocation as well attenuating the transcriptional programs driven by NF-κB and AP-1 (Fig. 7B).

[00128] Therefore, the inventors have found that DNAJB3 has a protective role in mitigating metabolic stress by binding to JNK1 and IKKβ enzymes and abrogating their activation in response to harmful stressors. DNAJB3 has also a positive role in improving glucose uptake at least in part by enhancing Glut4 translocation to the plasma membrane in C2C12. The inventors have found DNAJB3 has a physiological role in glucose metabolism and insulin signaling. Identifying small molecules that induce the expression DNAJB3 or recapitulate its function could be leveraged as a possible novel strategy for the control and management of metabolic defects leading to IR andT2D.

[00129] EXAMPLE 2

[00130] The inventors further assessed the effect ALA treatment on the endogenous expression of DNAJB3 in metabolically relevant cells and determined the significance of such

an effect on other forms of metabolic stress that trigger IR as well as on glucose uptake. The inventors found that ALA triggers a significant increase in the expression of DNAJB3 in C2C12 and HepG2 cells. Given the modulatory effect of ALA on ER stress and glucose uptake, the inventors investigated the significance of such activation on ER stress; one of the key hallmarks of obesity induced IR and T2D. ALA pre-treatment significantly reduced the expression of ER stress markers namely, GRP78, XBP1, XBP1s and ATF4 in response to both tunicamycin and glucolipotoxicity. In functional luciferase-based assays, ALA treatment abrogated significantly the tunicamycin-mediated transcriptional activation of ATF6 while stimulating insulin-stimulated glucose uptake. Of important relevance, knocking down the expression of DNAJB3 with siRNA abolished the protective effect of ALA on tunicamycin-induced ER stress, suggesting thus that DNAJB3 is a key mediator of ALA-alleviated tunicamycin and gucolipotoxicity-induced ER stress. Furthermore, the effect of ALA on insulin-stimulated glucose uptake is reduced significantly in C2C12 cells transfected with DNAJB3 siRNA. Together, the results suggest that DNAJB3 is a molecular target through which ALA alleviates ER stress and improve glucose uptake.

[00131] **Reagents.** Anti-DNAJB3 antibody was purchased from Proteintech (Proteintech Group, Inc., Chicago, IL). Anti-HSP72 antibody was purchased from ENZO (ENZO Life Sciences, Inc., Farmingdale, NY). Anti-GRP78 and anti-γ-Tubulin were purchased from Abcam (Abcam, Cambridge, UK). Anti-Actin and horseradish peroxidase-conjugated antibodies were purchased from Cell Signaling (Cell Signaling Technology, Inc., Danvers, MA). ALA, tunicamycin, palmitic acid, H_2O_2 and insulin were purchased from Sigma (Sigma-Aldrich, St. Louis, MO). C2C12 and HepG2 were purchased from ATCC (ATCC, Manassas, VA). Fluorescently labeled D-glucose analog (2-NBDG) was purchased from Cayman (Cayman, Ann Arbor, MI). Reporter plasmid carrying five copies of ATF6 binding site upstream of the Luc2P reporter gene was described previously. Scrambled and specific siRNA were purchased from Dharmacon (Dharmacon Inc., Lafayette, CO). Lipofectamine 3000 and lipofectamine RNAiMAX were purchased from Invitrogen (Invitrogen, Carlsbad, CA). Bright Glo Luciferase Assay kit was purchased from Promega (Promega Corporation, Madison, WI). PureLinkTM RNA Minikit and High-Capacity cDNA Reverse Transcription Kit were purchased from Invitrogen (Invitrogen, Carlsband, CA).

[00132] **Cell culture silencing RNA and transient transfections.** C2C12 and HepG2 cells were maintained in DMEM supplemented with 10% FBS and 1% penicillin/streptomycin at 37°C and 5% CO_2. Differentiation of C2C12 from myoblasts to myotubes was done by

replacing FBS with 2% horse serum with a daily change of the media for 5 days. For heat shock induction, ~85% confluent cells were incubated for 1h at 43°C followed by a 4h recovery at 37°C and then harvested. For the effect of ALA on ER stress induced by glucolipotoxicity, cells were challenged with 25 mM of glucose and 400 uM of palmitate for overnight and treated with ALA or vehicle for 24h and afterwards, harvested for RNA extraction. Lipofectamine 3000 and RNAiMAX lipofectamine were used for transient DNA and siRNA transfection, respectively as recommended by the manufacturer. We used a smart pool Accell siRNA targeting DNAJB3 and Accell non-targeting control at 20 nM each. All the functional assays were analyzed at least in triplicate and a minimum of three independent experiments.

[00133] **Luciferase assays.** C2C12 and HepG2 were grown in 100 mm petri dish and at ~80% confluence, they were transfected with 7.5 μg of the reporter plasmid using lipofectamine 3000 and incubated overnight at 37°C. On next day, they were plated on 96-well plates at 1.104 cells/well in complete DMEM media containing 0.3 mM ALA or vehicle. After 8h of incubation, cells were stimulated 0.5 μg/ml tunicamycin or vehicle and incubated at 37°C for overnight and then harvested for luciferase assays using the Bright Glo Luciferase Assay kit. To investigate if the effect of ALA on ER stress is mediated through DNAJB3, knocking down DNAJB3 in C2C12 cells was carried out with DNAJB3-siRNA or scrambled-siRNA or using lipofectmaine RNAiMAX protocol. The following day cells were transfected with 7.5 μg ATF6 reporter plasmid using Lipofectamine 3000 and incubated overnight at 37°C. Afterward, cells were then plated in 96-well plate at 1. 104 cells/well and pre-treated with ALA flowed by tunicamycin stimulation and luciferase activity.

[00134] **Measurement of gene expression by real-time PCR (RT-PCR).** RNA was extracted from treated cells using PureLinkTM RNA Minikit as instructed by the manufacturer. It was then converted to cDNA using High-Capacity cDNA Reverse Transcription Kit and analyzed by RT-PCR on QuantStudio 6 Flex system using SYBR Green (ThermoFisher, Waltham, MA). Relative expression was calculated by the comparative ΔΔCT method. GAPDH and actin genes were used as internal controls. The sequence of the primers is listed in Table 2 below.

[00135] **Table 2**

Gene	Species	Forward	Reverse
DNAJB3	Mouse	5′-AGGGGCTGTACCCTTCTCTA-3′	5′-AGTTTCCTGGAGAACCGAAG-3′
SOD1	Mouse	5′-GAGAGGCATGTTGGAGACCT-3′	5′-CCACCTTTGCCCAAGTCATC-3′
Catalase	Mouse	5′-AGGAGGCAGAAACTTTCCCA-3′	5′-GGCCCTGAAGCATTTTGTCA-3′

GPX1	Mouse	5′-ATCAGTTCGGACACCAGGAG-3′	5′-GATGTACTTGGGGTCGGTCA-3′
ATF4	Mouse	5′-GGGTTCTGTCTTCCACTCCA-3′	5′-AAGCAGCAGAGTCAGGCTTTC-3′
GRP78	Mouse	5′-AATTTCTGCCATGGTTCTCA-3′	5′-AGCATCTTTGGTTGCTTGTC-3′
XBP1	Mouse	5′-TCCCCAGAACATCTTCCCAT-3′	5′-ACATGACAGGGTCCAACTTG-3′
sXPB1	Mouse	5′-CTGAGTCCGAATCAGGTGCAG-3′	5′-GTCCATGGGAAGATGTTCTGG-3′
HSF1	Mouse	5′-GCTCAACATGTATGGCTTCC-3′	5′-GCTGGTCACTTTCCTCTTGA-3′
HSP70	Mouse	5′-TCTCCTGTCTTGTCCGAGAG-3′	5′-ATGCTGACTTGACCTTGAGC-3′
HSP72	Mouse	5′-GACAAGAAGAAGGTGCTGGA-3′	5′-TGGTACAGCCCACTGATGAT-3′
HSP90	Mouse	5′-TGAAACTGCTCTGCTCTCCT-3′	5′-CTCCTCTGCAGTGACCTCAT-3′
PGC1α	Mouse	5′-CACCAAACCCACAGAAAACAG-3′	5′GGG TCAGAGGAAGAGATAAAGTTG-3′
TFAM	Mouse	5′-GCTTGGAAAACCAAAAAGAC-3′	5′-CCCAAGACTTCATTTCATT-3′
PPARγ	Mouse	5′-GATGTCTCACAATGCCATCAG-3′	5′-TCAGCAGACTCTGGGTTCAG-3′
PPARα	Mouse	5′-AACATCGAGTGTCGAATATGTGG-3′	5′-CCGAATAGTTCGCCGAAAGAA-3′
Cytochrome C	Mouse	5′-CTGTGGAAAAGGGAGGCAAG-3′	5′-CACCTGGTAATTCTGCACTGG-3′
GAPDH	Mouse	5′-CTGGAGAAACCTGCCAAGTA-3′	5′-AGTGGGAGTTGCTGTTGAAG-3′
Actin	Mouse	5′-AAGAGCTATGAGCTGCCTGA-3′	5′- GATGCCACAGGATTCCATAC-3′

[00136] **Preparation of whole cell lysate and western blot analysis.** Whole protein extracts were prepared from treated cells using RIPA buffer 50 mM Tris·HCl, pH 7.5, 150 mM NaCl, 1% Triton X-100, 1 mM EDTA, 0.5% sodium deoxycholate and 0.1% SDS). Protein concentration was determined by the Bradford method using γ-globulin as a standard, and 40-80 μg of proteins were resolved on 10% SDS-PAGE gels. Proteins were then transferred onto PVDF membranes, blocked with 5% nonfat dried milk in Tris-buffered saline containing 0.05% Tween 20 (TBST) for 1h, and then probed with the primary antibody for overnight at 4°C. β-Actin and γ-Tubulin were used as internal controls. After washing, the membranes were incubated with horseradish peroxidase-conjugated secondary antibody for 2h. Protein bands were visualized by chemiluminescence and the images were captured using the ChemiDoc XRS+ system (Bio-Rad, Hercules, CA). For densitometric analysis, the intensity of the bands was determined using ImageJ software.

[00137] **Glucose uptake assay.** C2C12 cells at 80% confluence in 100 mm petri dishes were pre-treated with either 0.3mM ALA or vehicle for 8h and then, the media was replaced with glucose free media, containing either ALA or vehicle, for overnight starvation. The next day, the culture media was replaced with glucose free culture media containing Fluorescent tagged D-glucose analog (2-NBDG) at a concentration of 150 μg/ml with or without insulin 100nM and incubated for 1h at 37°C. Cells were then washed with Cell-Based Assay Buffer and

transferred to 96-well assay plate at 1.104 cells/well. Finally, fluorescence was quantified on Glomax Multi+ Microplate Multimode Reader (Promega, Madison, WI). Monitoring glucose uptake in C2C12 where the expression of DNAJB3 has been silenced was done by transfecting cells with DNAJB3-siRNA or scrambled control and after 2 days, cells were pre-treated with ALA for 8h and the media was changed to glucose free media with ALA and starvation and glucose uptake was carried out as described above.

[00138] **Statistical analysis.** Results are presented as means ± SEM and were plotted using GraphPad (Prism v7, La Jolla, CA). One-way ANOVA was used for comparison of the groups with post-hoc Tukey's test or the Student t test, as appropriate. A P-value <0.05 was considered statistically significant.

[00139] **ALA induces the endogenous expression of DNAJB3.** It has been shown previously that ALA mediates its beneficial effects by activating the HSR. However, these investigations have focused on a limited set of HSPs; namely HSP25, HSP60, HSP72, HSF1 and GRP75. The in vivo and in vitro investigations confirmed a novel role of DNAJB3 in reducing metabolic stress, improving insulin signaling and promoting glucose uptake. These findings suggest that DNAJB3 may represent a relevant therapeutic target against IR and T2D. The investors then assess the effect of ALA on the endogenous expression of DNAJB3 together with other key representative genes of the HSR.

[00140] Figs. 11A-11E show ALA induces the endogenous expression of DNAJB3 in C2C12 and HepG2 cells. Fig. 11A shows RT-PCR data showing the effect of 0.3 mM ALA for 24h on the expression of representative components of the heat shock response in C2C12 cells. Figs. 11B-11C show dose response effect of ALA on the expression of DNAJB3 mRNA (Fig. 11B) and protein (Fig. 11C) in C2C12 cells. Full-length blots are shown in Fig. 16. Fig. 16 shows that ALA induces the endogenous expression of DNAJB3 in C2C12cells. Cells were treated for 24h with increasing amounts of ALA. The levels of DNAJB3 protein were detected by western blot. γ-Tubulin was used as internal control.

[00141] Fig. 11D shows ALA at 0.3 mM for 24h also increases the expression of DNAJB3 mRNA in HepG2 cells. Fig. 11E shows heat shock treatment induces the expression of DNAJB3 mRNA. HSP72 was used as a positive control. Ethanol was used at 0.25% as a vehicle. * P<0.05; ** P< 0.01; *** P<0.001.

[00142] Data displayed in Fig. 11A confirmed indeed a significant increase (at least 4-fold increase) in the expression of DNAJB3 mRNA in C2C12 in response to treatment with 0.3 mM

ALA ($P<0.001$). Under the same experimental conditions, it was confirmed that the positive effect of ALA on modulating the expression of other heat shock related genes, although with different degrees, but the highest induction was observed for DNAJB3, flowed by HSP72 (Fig. 1A; $P<0.05$). The inventors did a time course and a dose response with ALA and monitored the expression of DNAJB3 mRNA and protein. Data displayed in Figs. 11B and 11C indicate that ALA induces the expression of DNAJB3 mRNA (Fig. 1B) and protein (Fig. 11C) in a time course-dependent manner. The inventors also examined the effect of ALA on HepG2 cells and observed a significant induction of DNAJB3 mRNA (Fig. 11D; $P<0.05$). Finally, the inventors compared the magnitude of ALA effect on the expression of DNAJB3 and HSP72 with heat shock treatment and the results are shown in Fig. 11E. As indicated, heat treatment for 1h at 43°C and recovery at 37°C for 4h resulted in a similar increase in the expression of DNAJB3 mRNA as compared to ALA ($P<0.001$). The expression of HSP72 was also increased, albeit to a lower level than that caused by heat (more than 30-fold) in response to heat shock than to ALA treatment ($P<0.01$). The induction of both DNAJB3 and HSP72 has been confirmed by western blot analysis (data not shown). Taken together, these data indicate clearly that ALA modulates positively the endogenous expression of DNAJB3 both at mRNA and protein levels.

[00143] **Pre-treatment of C2C12 cells with ALA alleviates tunicamycin-induced ER stress.** The contribution of persistent ER stress to the pathogenesis of IR and T2D is well established. Several studies reported the effectiveness of ALA in alleviating ER stress; however, none of these studies examined the effect ALA in skeletal muscle cells. The inventors therefore investigated whether pre-treatment of C2C12 cells with ALA could mitigate tunicamyin-induced ER stress by measuring the expression and activity of known ER stress markers.

[00144] Figs. 12A-12E show ALA alleviates tunicamycin and glucolipotixicity-induced ER stress. Figs. 12A-12B show pre-treatment of C2C12 cells with 0.3 mM ALA abolishes significantly the mRNA expression of classical ER stress markers in response to both tunicamycin (Fig. 12A) and glucolipotoxicity (Fig. 12B) conditions. Fig. 12C show western blot confirming the effect of ALA on tunicamycin-induced expression of GRP78 protein. Full-length blots are shown in Fig. 17. Fig. 17 shows the ALA alleviates tunicamycin-induced expression of GRP78 protein in C2C12 cells as monitored by western blot. β-Actin was used as internal control.

[00145] Figs. 12D-12E show ALA also reduces ATF6-dependent luciferase activity in response to tunicamycin using a functional luciferase-based assay both in C2C12 (Fig. 12D)

and HepG2 (Fig. 12E) cells. Ethanol and DMSO were used at 0.25% as vehicles for ALA and tunicamycin, respectively. * P<0.05; ** P< 0.01; *** P<0.001.

[00146] Data displayed in Figs. 12A-12E indicate that overnight treatment of C2C12 cells with 0.5 µg/ml tunicamycin led to a marked increase in the endogenous expression of GRP78, XBP1 and it spliced form sXBP1 and ATF4 as compared to the vehicle (Fig. 12A). In cells pre-treated with ALA, there was a significant reduction in tunicamycin-mediated effect on those markers (Fig. 12A). The ability of ALA to alleviate ER stress has been confirmed in cells challenged to glucolipotoxicity (Fig. 12B). At the protein level, the inventors confirmed the inhibitory effect of ALA on tunicamycin-induced activation of GRP78 protein (Fig. 12C). To complement these findings, the inventors used a functional luciferase-based assay to examine the effect of ALA on the activity of ATF6 in response to tunicamycin. As shown in Fig. 12D, a 5-fold increase in ATF6-dependent luciferase activity in response to 0.5 µg/ml tunicamycin was consistently observed. Pre-treatment of cells with ALA reduced significantly the ATF6-dependent luciferase activity (Fig. 12D; P < 0.001). In HepG2 cells, a similar pattern was also observed (Fig. 12E), although the magnitude of tunicamycin effect was less pronounced than in C2C12. These results confirm the beneficial role of ALA in attenuating tunicamycin-induced ER stress in skeletal muscle and in liver cells.

[00147] **ALA stimulates the expression of mitochondrial markers and the oxidative stress scavenging system in C2C12 cells.** Dysfunction of mitochondria and/or its biogenesis was linked to IR and T2D (Gonzalez-Franquesa, A. & Patti, M. E. Insulin Resistance and Mitochondrial Dysfunction. *Advances in experimental medicine and biology* **982**, 465-520, doi:10.1007/978-3-319-55330-6_25 (2017); Hesselink, M. K., Schrauwen-Hinderling, V. & Schrauwen, P. Skeletal muscle mitochondria as a target to prevent or treat type 2 diabetes mellitus. *Nature reviews. Endocrinology* **12**, 633-645, doi:10.1038/nrendo.2016.104 (2016); Pinti, M. V. *et al.* Mitochondrial dysfunction in type 2 diabetes mellitus: an organ-based analysis. *American journal of physiology. Endocrinology and metabolism* **316**, E268-e285, doi:10.1152/ajpendo.00314.2018 (2019); Szendroedi, J., Phielix, E. & Roden, M. The role of mitochondria in insulin resistance and type 2 diabetes mellitus. *Nature reviews. Endocrinology* **8**, 92-103, doi:10.1038/nrendo.2011.138 (2011)). One of the attractive features of ALA is its effect on promoting mitochondrial function and biogenesis. The inventors measured the expression of key representative mitochondrial marker genes in C2C12 in response to ALA.

[00148] Figs. 13A shows that ALA improves mitochondrial function. Fig. 13A shows that ALA treatment triggers a significant increase in the expression of TFAM (P<0.05), PPARγ and

its coactivator PGC1α ($P<0.001$), and cytochrome C ($P<0.05$). No significant effect was observed for PPARγ (Fig. 13A).

[00149] The inventors then examined the effect of ALA on modulating the mRNA expression of genes encoding for representative antioxidant enzymes; namely catalase, glutathione peroxidase (GPX1) and superoxide dismutase 1 (SOD1). Results displayed in Fig. 13B indicate a significant increase in the mRNA expression levels of catalase ($P<0.001$) both at basal level and after H2O2 treatment. A positive effect of ALA on the expression of SOD1 and GPX1 genes was observed but only under oxidative stress conditions (Fig. 11B; $P<0.05$).

[00150] **Silencing the expression of DNAJB3 abolished the beneficial effect of ALA on alleviating tunicamycin-induced ER stress.** The inventors found a negative regulation of DNAJB3 expression when ER stress is induced. Reciprocally, both basal and tunicamycin-induced ER stress are significantly reduced when DNAJB3 is overexpressed. This is suggestive of a mutual negative feedback regulation between DNAJB3 and ER stress. To get more insight in the possible role of DNAJB3 as a molecular determinant through which ALA mediates its beneficial effect on ER stress, the inventors knocked down the expression of DNAJB3 using siRNA and then, induced ER stress with tunicamycin in C2C12 cells pre-treated with ALA.

[00151] Figs. 14A-14C show silencing the expression of DNAB3 abolishes the protective effect of ALA on tunicamycin-induced ER stress. Fig. 14A shows knocking down the expression of DNAJB3 expression with 20 nM of specific siRNA blunted the endogenous expression of DNAJB3 in C2C12 cells. Actin gene was used as a reference control. Figs. 14B-14C show ALA fails to protect cells from tunicamycin-induced mRNA expression of ER stress markers (Fig. 14B) and ATF6-dependent luciferase activity (Fig. 14C) in cells transfected with siRNA specific for DNAJB3.

[00152] Silencing the expression of DNAJB3 with specific siRNA abrogated effectively the expression of DNAJB3 mRNA in C2C12 cells (Fig. 14A; $P<0.001$). The ability of ALA to reduce ER stress when the expression of DNAJB3 is silenced is illustrated in Figs. 14B and 14C. As shown, DNAJB3 siRNA abolished the beneficial effect of ALA on attenuating tunicamycin-induced ER stress marker genes as compared to scrambled siRNA control (Fig. 14B). Consistent with these findings, ALA treatment significantly reduced the ATF6-dependent luciferase activity in response to tunicamycin as compared to scrambled siRNA control (Fig. 14C; $P<0.01$). Together, these findings suggest that ALA attenuates ER stress, at least in part through DNAJB3.

[00153] **ALA-stimulated glucose uptake is significantly reduced in cells transfected with DNAJB3 si-RNA.** The inventors found that DNAJB3 has a positive effect on enhancing both basal and insulin-stimulated glucose uptake. The inventors assessed first the effect of ALA on glucose uptake in C2C12 and then, investigated whether DNAJB3 is involved in such effect.

[00154] Figs. 15A-15B show silencing the expression of DNAB3 abrogated the effect of ALA on enhancing glucose uptake in C2C12 cells. Fig. 15A shows effect of ALA on insulin-stimulated glucose uptake. Fig. 15B shows silencing the expression of DNAJB3 abrogated the effect of ALA on insulin-stimulated glucose uptake as compared to scrambled siRNA control. *** $P<0.001$.

[00155] Data displayed in Fig. 15A indicates that ALA enhanced insulin-stimulated glucose uptake by approximately 20% ($P<0.001$). In cells where the expression of DNAJB3 has been silenced, ALA failed to promote glucose uptake elicited by insulin (Fig. 15B; $P<0.001$).

[00156] Impaired expression of HSP25, HSP72 and DNAJB3, three important components of the HSR has been documented in diabetic patients and in experimental high fat diet animals in a manner that correlates negatively with the degree of IR. Consistent with this, interventions that activate the HSR; irrespective of the means to achieve it (i.e., heat therapy, physical exercise, mild electrical therapy, genetic overexpression and pharmacological drugs) showed a greater improvement in insulin sensitivity and glucose homeostasis. The inventors found a clear physiological role of DNAJB3 in mitigating metabolic stress and improving insulin signaling and glucose homeostasis in C2C12 skeletal muscle cells and 3T3-L1 adipocytes. In rat model of high fat-induced IR and glucose intolerance, the ability of ALA to prevent the decrease of HSP25 and HSP72 levels with effective improvement of insulin action and glycemic index has been reported. The inventors investigated the effect of ALA on the endogenous expression of DNAJB3 in metabolically relevant cells and the significance of such effect on ER stress and glucose uptake. It has be found that ALA: 1- induces the expression of DNAJB3 in C2C12 and HepG2 cell lines, 2- alleviates ER stress triggered by tunicamycin and glucolipotoxicity and improve glucose uptake, 3- knocking down the expression of DNAJB3 with siRNA abolished the beneficial effect of ALA in alleviating tunicamycin-induced ER stress and enhancing insulin-stimulated glucose uptake. Taken together, the inventors found DNAJB3 as a molecular determinant that mediates the beneficial effect of ALA in attenuating metabolic stress. The identification of DNAJB3 as a downstream target of ALA supports further the importance of the HSR in mitigating the key drivers of IR.

[00157] DNAJB3, previously known as MSJ-1 was initially described in mice as a gene involved in male reproduction, but given the presence of a highly conserved and functionally critical J-domain, the gene was subsequently named DNAJB3; a member of the DNAJ/HSP40 cochaperone family that acts as an obligate partner and critical regulator of the activity and substrate specificity of HSP70 chaperone. DNAJB members exert their role by stimulating the ATPase activity of HSP70 through their J-domain, thereby keeping the bound substrates in successive refolding cycles. The inventors found the novel *in vitro* role of DNAJB3 in insulin signaling and glucose metabolism. Based on this novel role, and given its importance in regulating the chaperone activity of HSP70, DNAJB3 represents a potential therapeutic target for diseases associated with IR and proteotoxicity. The finding of the current study; despite been carried out in vitro, is the first showing the druggability of DNAJB3 target with a relevant pharmacological drug.

[00158] In all living organisms, cells cope with various noxious conditions by inducing a dedicated set of anti-stress responses to ensure normal cellular homeostasis and any persistent dysregulation of these responses may lead to pathological disorders. The detrimental consequences of impaired HSR on the pathogenesis of IR and T2D are well established. This has been particularly the case for HSP25, HSP72, and DNAJB3. Given their ability to bind and inactivate JNK1 and IKKβ kinases, HSPs emerged as attractive therapeutic targets for obesity-induced IR and T2D. A positive effect of ALA on modulating various components of the HSR such as HSP25, HSP72 and HSF1 has been shown previously. However, the inventors are the first to find the effect of ALA effect on DNAJB3 expression. ALA treatment caused significant increase in DNAJB3 mRNA expression in C2C12 and HepG2 cells. Without being bound to the theory, the inventors believe that the most likely mechanism for HSPs induction would be activation of HSF1; the master transcription factor controlling the HSR. Under the experimental conditions, the inventors observed a slight, but significant increase in HSF1 mRNA levels in response to ALA (Fig. 11A) and this could play a role in DNAJB3 activation. Similar findings have been reported in streptozotocin-induced diabetic rat in response to ALA. By contrast, ALA supplementation showed no effect on HSF1 expression in the skeletal muscle of high fat fed rat model of IR, as well as under heat stress conditions in Caco-2 cells. The dose, route of administration, biological context and duration of treatment could explain the discrepancy between those studies. Moreover, the DNA-binding activity of HSF1 has been shown to be potentiated with SIRT1 deacetylase. Interestingly, SIRT1 expression is also positively regulated with ALA. Alternatively, ALA could control the expression through the

nuclear factor-erythroid 2 (Nrf2); another safeguard transcription factor that regulates the expression of anti-oxidant response genes, as well as HSR genes. In high fat diet-induced hepatic steatosis rat Goto-Kakizaki model, ALA prevented hepatic steatosis by incrementing antioxidant defense systems through Nrf2. Nrf2 executes its task by binding to the antioxidant response element (ARE) in the promoter region of its downstream target genes and subsequently drives their expression. Interestingly, both mouse and human DNAJB3 promoters have a putative ARE. Data show increased expression in DNAJB3 mRNA and protein in response to sulforaphane and resveratrol, two potent activators of Nrf2 (data not shown).

[00159] Another important finding of the inventors is the effect of ALA on tunicamycin-induced ER stress; a major trigger of IR and T2D. The ER is a dispersed organelle throughout the cell that performs important homeostatic functions related to proteostasis, lipid metabolism and calcium storage. These processes rely on the protein folding activity of chaperone machinery densely populated in the ER. Disruption of ER homeostasis occurs when the folding capacity of the ER fails to accommodate the overwhelming load of misfolded and unfolded proteins, leading thus to ER stress. This elicits a potent adaptive response known as the unfolded protein response (UPR); an acute mechanism that assists in restoring ER activity and reestablishing cellular homeostasis. However, sustained chronic UPR activation as a result of persistent (unresolved) ER stress has been implicated in a variety of metabolic disorders, including obesity, IR and T2D. By contrast, restoring ER homoeostasis either pharmacologically or genetically was shown to reverse IR and improve glucose homeostasis. In eukaryotic cells, the UPR is initiated by the activation of three ER stress canonical transducers that act in concert to restore ER homeostasis: PKR-like ER kinase (PERK), inositol-requiring enzyme-1α (IRE1α), and activating transcription factor-6 (ATF6). Under normal conditions, the luminal stress-sensing domain of PERK, IRE1α, and ATF6 interacts with GRP78 chaperone, however upon accumulation of unfolded proteins, GRP78 dissociates from these transducers, leading to their activation. Each of these transducers activates specific pathways and collectively leads to decreased overall protein synthesis, enhanced ER folding capacity and increased degradation of misfolded proteins, resulting in either recovery of ER homeostasis or cell death. Tunicamycin is a well-known ER stress inducer both *in vitro* and *in vivo*. The results show that tunicamycin and glucolipotoxicity lead to a marked increase in the expression of the genes of the UPR system, namely GRP78, ATF4, XBP and its spliced form sXBP1 (Figs. 12A-12E). Consistent with this, we observed also an increase in the luciferase activity driven by ATF6 in response to tunicamycin (Figs. 12A-12E). The inventors found that

tunicamycin-induced increase in GRP78, ATF4, XBP and sXBP1s mRNA expression was impeded by ALA (Figs. 12A-12E). At the protein level, the inventors measured the effect of ALA on tunicamycin-mediated expression of GRP78 protein and confirmed the RT-PCR data (Fig. 12C). In functional assays, tunicamycin-mediated ATF6 activation was significantly reduced with ALA (Figs. 12D-12E). These findings have been further confirmed in C2C12 cells subjected to glucolipotoxicity (Fig. 12B).

[00160] Another important finding by the inventors is that DNAJB3 is one of the molecular targets through which ALA attenuates ER stress. Defects in the HSR and persistent ER stress are one of the critical aberrations underlying IR and T2D. Alleviation of ER stress and enhancement of the HSR have previously been considered as attractive potential therapeutic pathways against several chronic diseases. In L6 cells, the ability of ALA to prevent anisomycin-mediated JNK activation is abolished upon inhibition of the HSR with KNK437 drug, supporting thus a role of the HSR as mediator of the metabolic actions elicited by ALA. The inventors found the negative regulation of DNAJB3 expression when ER stress is induced. The inventors also found a reciprocal effect of DNAJB3 on both basal and tunicamycin-induced ER stress. This is suggestive of a mutual negative feedback regulation between DNAJB3 and ER stress that provides a functional crosstalk between both stress pathways. To get more insight in the possible role of DNAJB3 as a molecular determinant through which ALA alleviates ER stress, the inventors silenced the expression of DNAJB3 using siRNA and then, assessed the ability of ALA to reduce ER stress in response to tunicamycin. The data show that DNAJB3 siRNA abolished the beneficial effect of ALA on tunicamycin-induced ER stress marker genes as compared to scrambled siRNA control (Fig. 14B; $P<0.05$). Consistent with these findings, the effect of ALA on reducing ATF6 activity in response to tunicamycin was also reduced significantly as compared to scramble siRNA control (Fig. 14C; $P<0.05$). Together, these findings suggest that ALA attenuates ER stress, at least in part through DNAJB3.

[00161] It is not clear whether DNAJB3 exerts a direct effect on ER stress or indirectly via other pathways. The close link between ER stress and mitochondrial homeostasis has been described. In HepG2 cells, ALA prevented ER stress-induced IR by enhancing mitochondrial function, but surpisingly; it failed to abrogate the expression of tunicamycin-induced ER stress markers. The inventors observed a positive correlation between DNAJB3 levels and maximum oxygen consumption in human subjects. In C2C2 cells, overexpression of DNAJB3 stimulated the expression of conventional markers of mitochondrial biogenesis and function such as

TFAM, PGC1α, PPARγ and OXPHOS subunits (unpublished data). Interestingly, this pattern was also observed in the current study. Specifically ALA supplementation increased the mRNA levels of TFAM, PGC1α, PPARγ and cytochrome C in C2C12 cells (Fig. 13A); consistent with previous findings in other cellular systems. It is possible that DNAJB3 attenuates ER stress by promoting mitochondrial homeostasis. In this context, it will be important to assess the effect of DNAJB3 on ER stress under the conditions where the mitochondrial function is impaired (i.e., oligomycin). Alternatively, DNAJB3 could physically interact with one or several transducers of the UPR and trigger an inhibitory effect on their respective activities. This has been particularly the case for ERdj4/DNAJB9; another member of DNAJB family that prevents the oligomerization of IRE1α transducer by promoting complex formation between the luminal GRP78 and luminal stress-sensing domain of IRE1α and thereby repressing its enzymatic activity.

[00162] ALA may also attenuate ER stress via reduction of the oxidative stress through stimulating the anti-oxidant response genes as previously reported. ER stress and oxidative stress are important mechanisms of IR. The inventors found the ability of DNAJB3 to mitigate oxidative stress induced with H2O2. In the current study, ALA treatment stimulated the expression of the oxidative stress scavenging genes Catalase, SOD1 and GPx-1 in response to H2O2 (Fig. 13B), replicating previous findings in C2C12 cells. To investigate whether the beneficial effects of ALA on ER stress and oxidative stress is associated with improved glucose and insulin metabolism, C2C12 cells were treated with ALA and insulin-induced glucose uptake was performed. The results showed a significant increase in insulin-stimulated glucose uptake following ALA treatment, similar to a pattern following DANJB3 overexpression in C2C12 cells.

[00163] To examine the specificity of DNAJB3 on the effect of ALA on insulin-stimulated glucose uptake, the ininventors silenced the expression of DNAJB3 using siRNA and then, assessed the effect of ALA on glucose uptake. The data show that inhibition of DNAJB3 abolished the beneficial effect of ALA on insulin-stimulated glucose uptake; suggesting that ALA improves glucose uptake through DNAJB3.

[00164] Therefore, the inventors have found stimulatory effect of ALA on the expression of DNAJB3 in C2C12 and HepG2. More importantly, the inventors have found a novel mechanism by which ALA modulates ER stress and glucose uptake.

[00165] Further embodiments can be found in "DNAJB3 attenuates metabolic stress and promotes glucose uptake by eliciting Glut4 translocation," *Scientific Reports*, (2019) 9:4772, which is incorporated by reference.

[00166] It should be understood that various changes and modifications to the presently preferred embodiments described herein will be apparent to those skilled in the art. Such changes and modifications can be made without departing from the spirit and scope of the present subject matter and without diminishing its intended advantages. It is therefore intended that such changes and modifications be covered by the appended claims.

CLAIMS

1. A biomarker for diagnosis of a chronic condition linked to insulin resistance (IR), the biomarker comprising a polypeptide encoded by DNAJB3, wherein the chronic condition is selected from the group consisting of diabetes, metabolic syndrome and their complications.

2. The biomarker of claim 1, wherein overexpression of the DNAJB3 enhances basal and insulin-stimulated glucose uptake.

3. The biomarker of claim 1, wherein overexpression of DNAJB3 elicits Glut4 translocation to the plasma membrane in C2C12 cells.

4. The biomarker of claim 1, wherein overexpression of DNAJB3 alleviates basal ER stress and enhances the oxidative stress scavenging system.

5. The biomarker of claim 1, wherein DNAJB3 abrogated both JNK1 and IKKβ pathways.

6. The biomarker of claim 1, wherein DNAJB3 suppressed TNF-α-mediated IL-6 promoter activation and mRNA expression.

7. A method comprising using a biomarker comprising a polypeptide encoded by DNAJB3 to diagnose a chronic condition linked to IR, wherein the chronic condition is selected from the group consisting of diabetes, metabolic syndrome and their complications.

8. The method of claim 7 comprising using the biomarker as an early molecular signature to detect early cellular, molecular and biochemical aberrations underpinning IR and diabetes.

9. The method of claim 7, wherein overexpression of the DNAJB3 enhances basal and insulin-stimulated glucose uptake.

10. The method of claim 7, wherein overexpression of DNAJB3 elicits Glut4 translocation to the plasma membrane in C2C12 cells.

11. The method of claim 7, wherein overexpression of DNAJB3 alleviates basal ER stress and enhances the oxidative stress scavenging system.

12. The method of claim 7, wherein DNAJB3 abrogates both JNK1 and IKKβ pathways.

13. The method of claim 7, wherein DNAJB3 suppresses TNF-α-mediated IL-6 promoter activation and mRNA expression.

14. A pharmaceutical composition comprising ALA, wherein the pharmaceutical composition is configured to prevent and/or treat a chronic condition linked to IR, and the chronic condition is selected from the group consisting of diabetes, metabolic syndrome and their complications.

15. A method for preventing and/or treating a chronic condition linked to IR in a subject in need of same, the method comprising administering a composition comprising ALA to the subject, wherein the chronic condition is selected from the group consisting of diabetes, metabolic syndrome and their complications.

16. The method of claim 15 comprising using the ALA to induce the endogenous expression of DNAJB3 gene/protein or recapitulate the activity of DNAJB3.

17. The method of claim 15 comprising pre-treatment of C2C12 cells with the ALA to alleviate tunicamycin-induced ER stress.

18. The method of claim 15 comprising using the ALA to stimulate the expression of mitochondrial markers and the oxidative stress scavenging system in C2C12 cells.

FIG. 1A

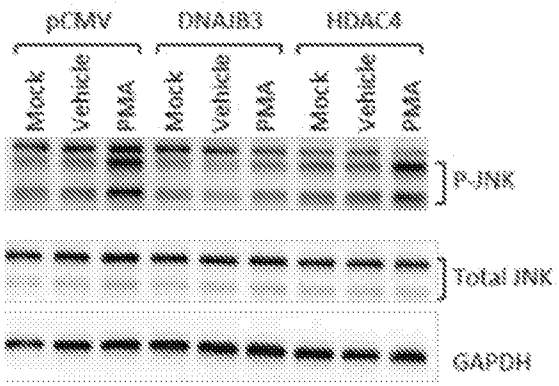
pCMV
DNAJB3
HDAC4
Mock
Vehicle
PMA
Mock
Vehicle
PMA
Mock
Vehicle
PMA
P-JNK
Total JNK
GAPDH

FIG. 1B

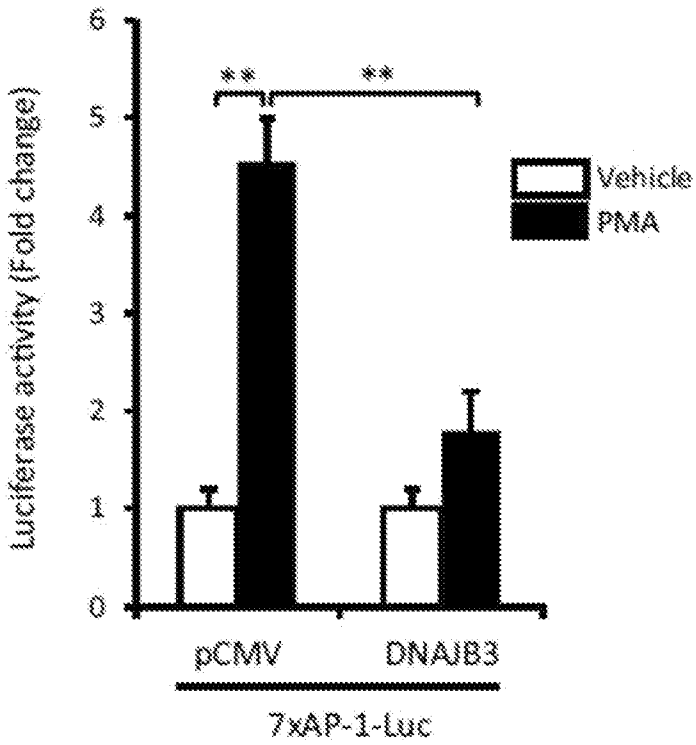
Luciferase activity (Fold change)
0
1
2
3
4
5
6
**
**
Vehicle
PMA
pCMV
DNAJB3
7xAP-1-Luc

FIG. 2A

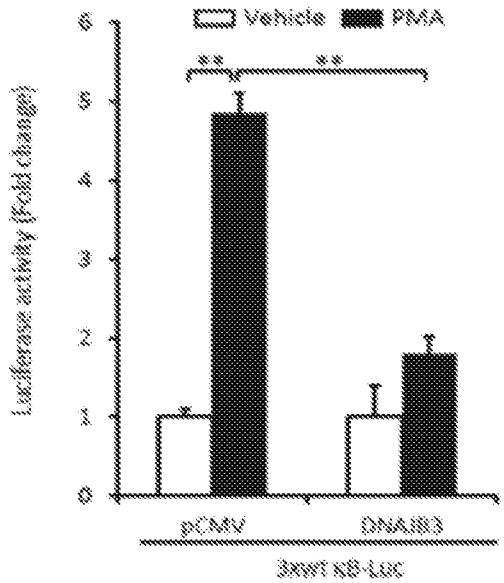
Vehicle
PMA
**
**
Luciferase activity (Fold change)
6
5
4
3
2
1
0
pCMV
DNAJB3
3xwt κB-Luc

FIG. 2B

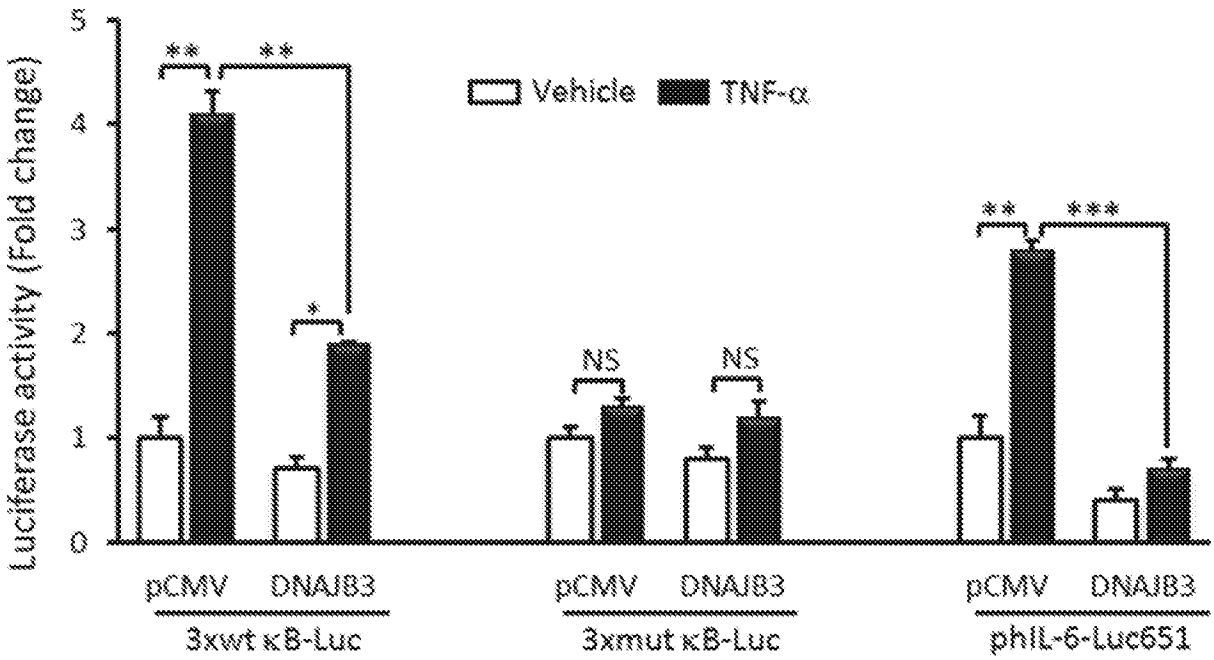
Luciferase activity (Fold change)
5
4
3
2
1
0
Vehicle
TNF-α
**
**
*
NS
NS
**
***
pCMV
DNAJB3
3xwt κB-Luc
pCMV
DNAJB3
3xmut κB-Luc
pCMV
DNAJB3
phIL-6-Luc651

FIG. 3A

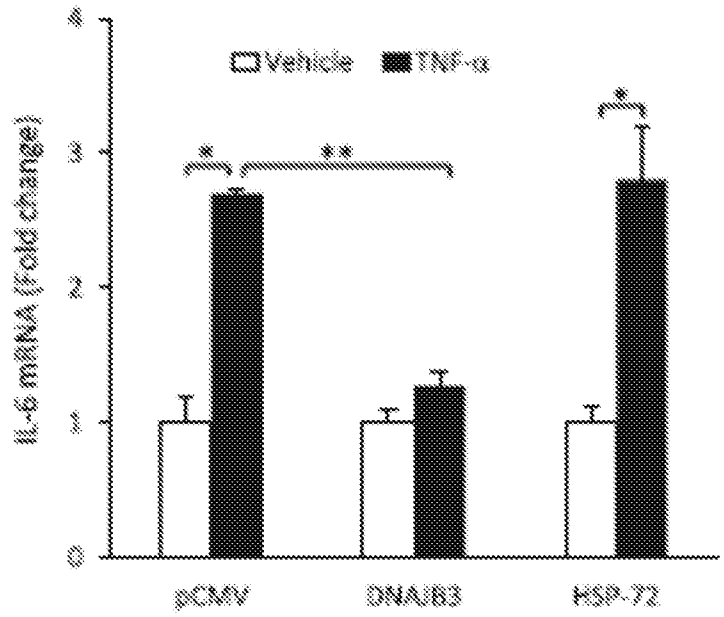
Vehicle
TNF-α
IL-6 mRNA (Fold change)
0
1
2
3
4
*
**
*
pCMV
DNAJB3
HSP-72

FIG. 3B

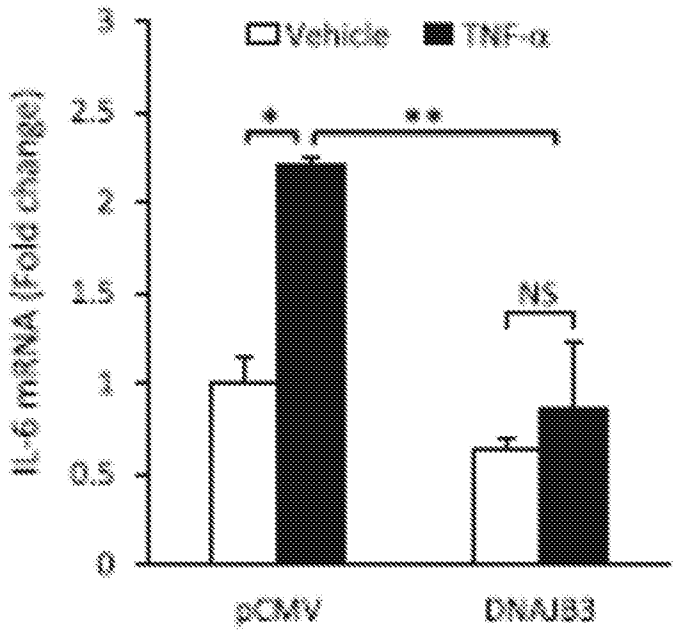
Vehicle
TNF-α
IL-6 mRNA (Fold change)
0
0.5
1
1.5
2
2.5
3
*
**
NS
pCMV
DNAJB3

FIG. 3C

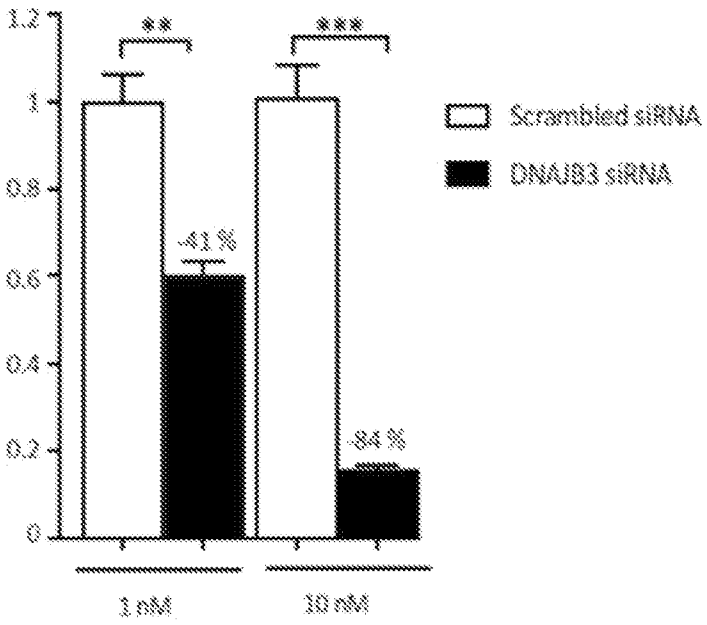
1.2
1
0.8
0.6
0.4
0.2
0
**
***
-41 %
-84 %
Scrambled siRNA
DNAJB3 siRNA
1 nM
10 nM

FIG. 3D

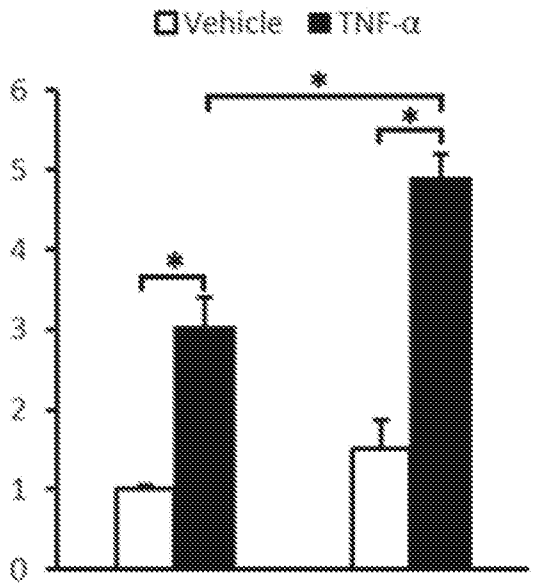
Vehicle
TNF-α
6
5
4
3
2
1
0
*
*
*

FIG. 3E

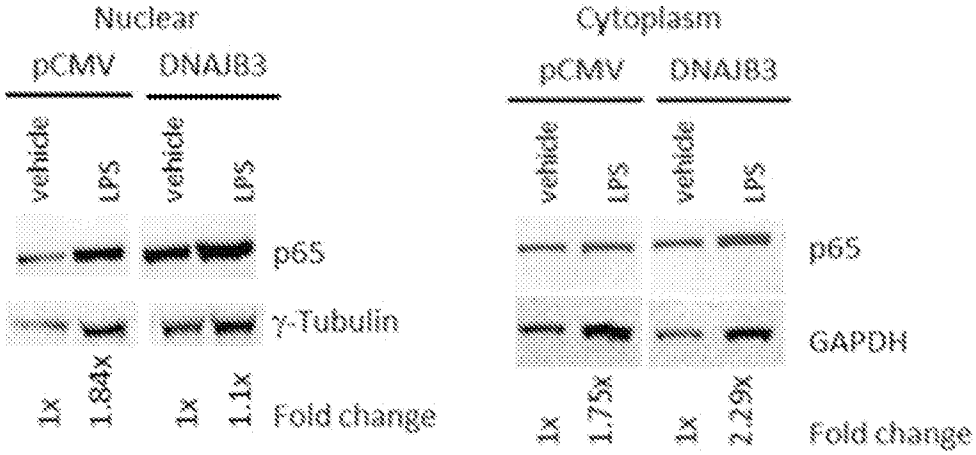
Nuclear
pCMV
DNAJB3
vehicle
LPS
vehicle
LPS
p65
γ-Tubulin
1x
1.84x
1x
1.1x
Fold change
Cytoplasm
pCMV
DNAJB3
vehicle
LPS
vehicle
LPS
p65
GAPDH
1x
1.75x
1x
2.29x
Fold change

FIG. 4A

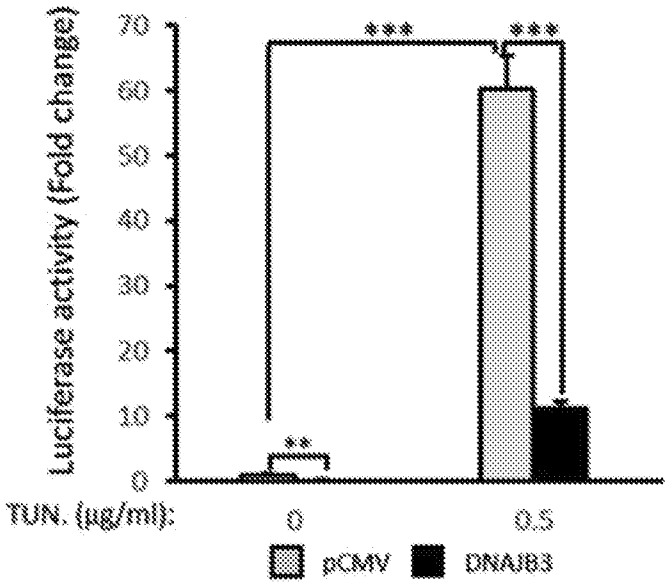
Luciferase activity (Fold change)
70
60
50
40
30
20
10
0
***
***
**
TUN. (μg/ml):
0
0.5
pCMV
DNAJB3

FIG. 4B

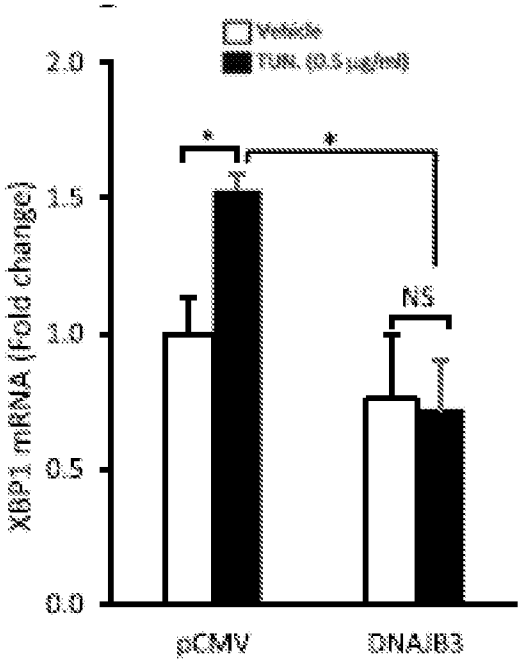
Vehicle
2.0
1.5
1.0
0.5
0.0
XBP1 mRNA (Fold change)
*
*
NS
pCMV
DNAJB3

FIG. 4C

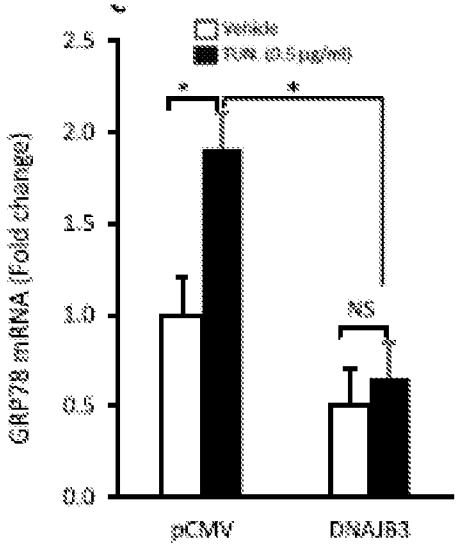
Vehicle
2.5
2.0
1.5
1.0
0.5
0.0
GRP78 mRNA (Fold change)
*
*
NS
pCMV
DNAJB3

FIG. 4D

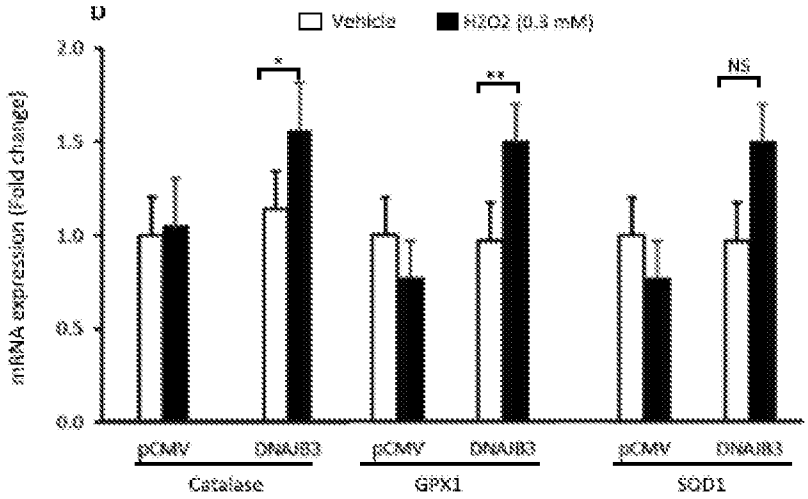
D
Vehicle
H2O2 (0.3 mM)
mRNA expression (Fold change)
3.0
2.5
2.0
1.5
1.0
0.5
0.0
*
**
NS
pCMV
DNAJB3
Catalase
GPX1
SOD1

FIG. 5A

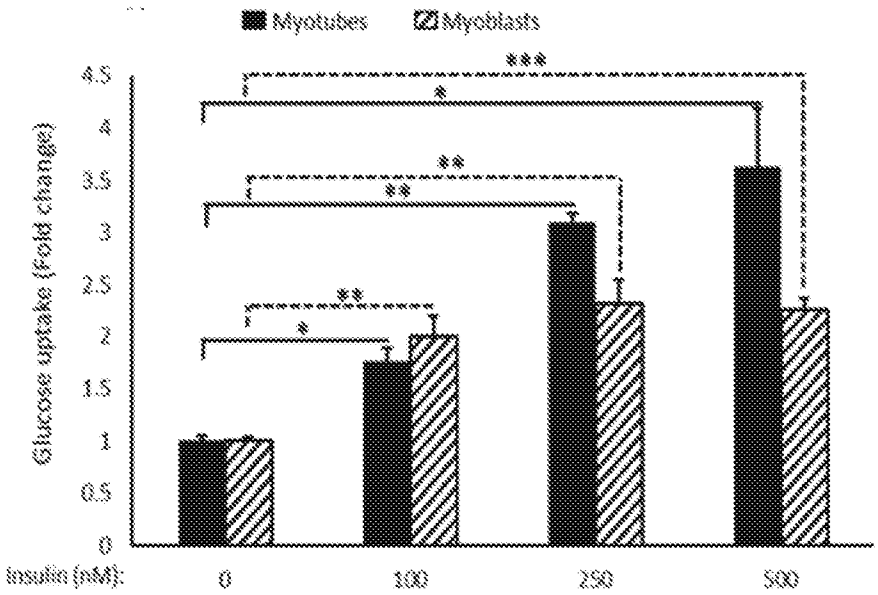
Myotubes
Myoblasts
Glucose uptake (Fold change)
4.5
4
3.5
3
2.5
2
1.5
1
0.5
0
***
*
**
**
**
*
Insulin (nM):
0
100
250
500

FIG. 5B

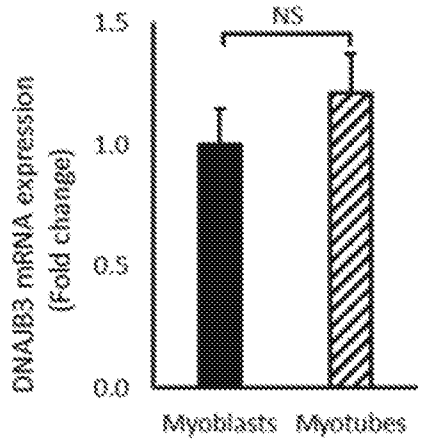
NS
1.5
1.0
0.5
0.0
DNAJB3 mRNA expression
(Fold change)
Myoblasts
Myotubes

FIG. 5C

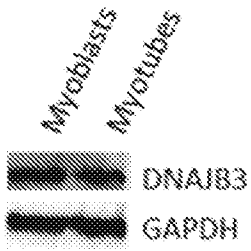
Myoblasts
Myotubes
DNAJB3
GAPDH

FIG. 5D

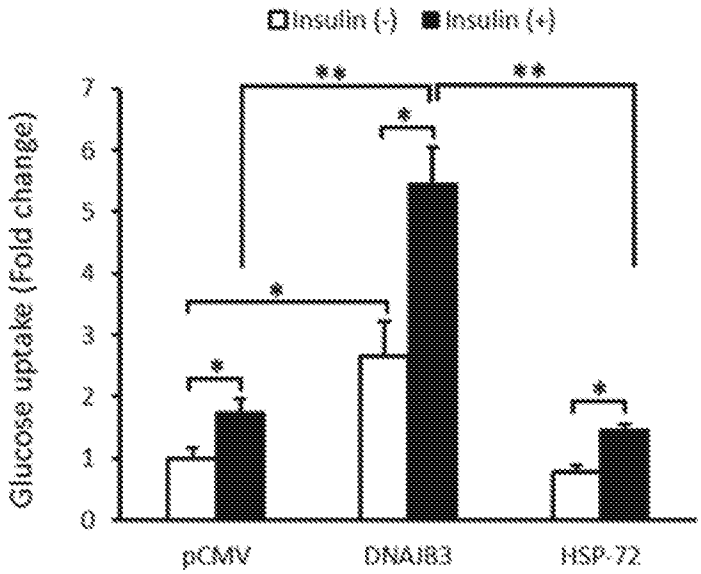
Insulin (-)
Insulin (+)
Glucose uptake (Fold change)
0
1
2
3
4
5
6
7
*
*
*
*
**
**
pCMV
DNAJB3
HSP-72

FIG. 5E

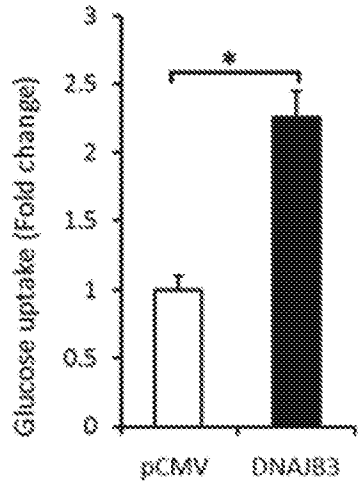
Glucose uptake (Fold change)
0
0.5
1
1.5
2
2.5
3
*
pCMV
DNAJB3

FIG. 5F

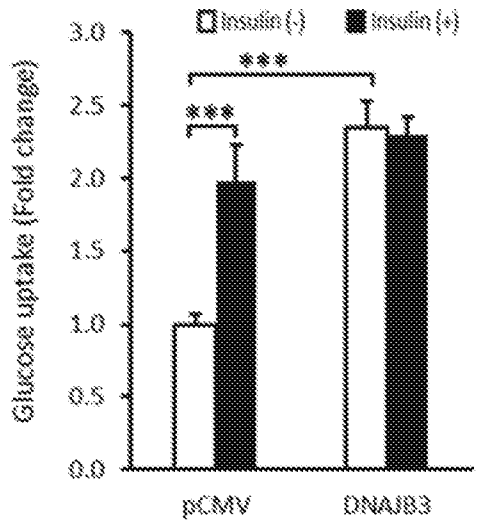
Insulin (-)
Insulin (+)
***
***
Glucose uptake (Fold change)
3.0
2.5
2.0
1.5
1.0
0.5
0.0
pCMV
DNAJB3

FIG. 5G

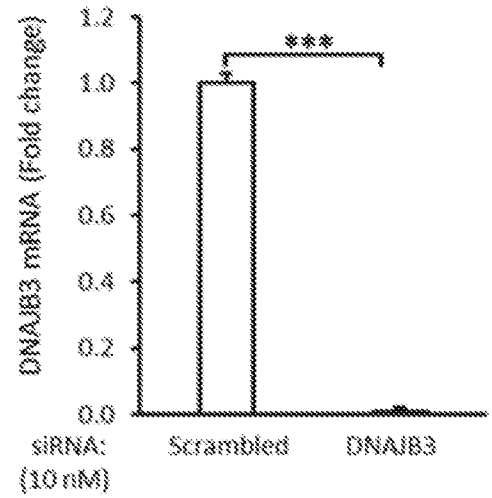
***
DNAJB3 mRNA (Fold change)
1.2
1.0
0.8
0.6
0.4
0.2
0.0
siRNA:
(10 nM)
Scrambled
DNAJB3

FIG. 5H

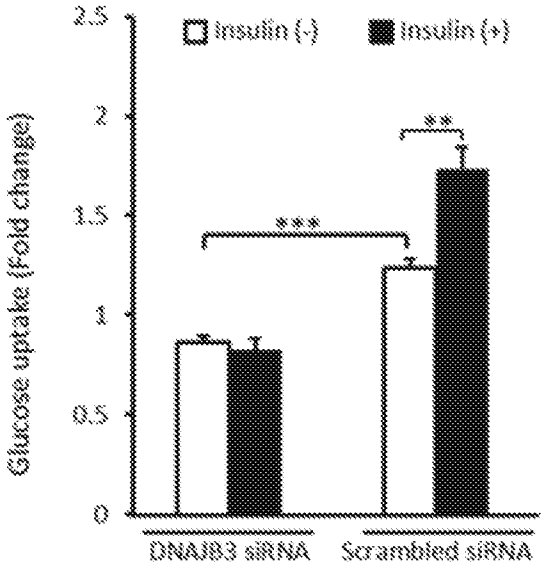
Insulin (-)
Insulin (+)
Glucose uptake (Fold change)
2.5
2
1.5
1
0.5
0
**
***
DNAJB3 siRNA
Scrambled siRNA

FIG. 6A

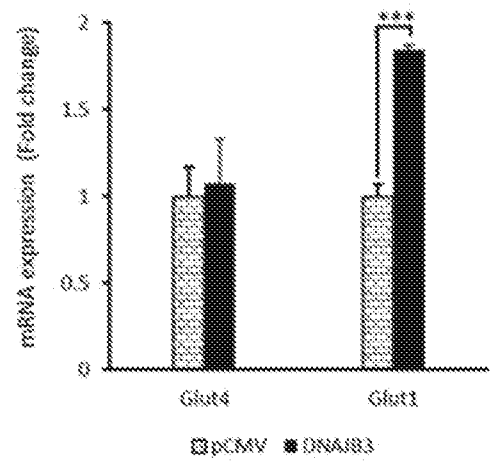
mRNA expression (Fold change)
2
1.5
1
0.5
0
***
Glut4
Glut1
pCMV
DNAJB3

FIG. 6B

FIG. 6C

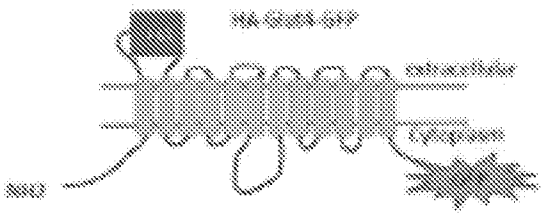

FIG. 6D

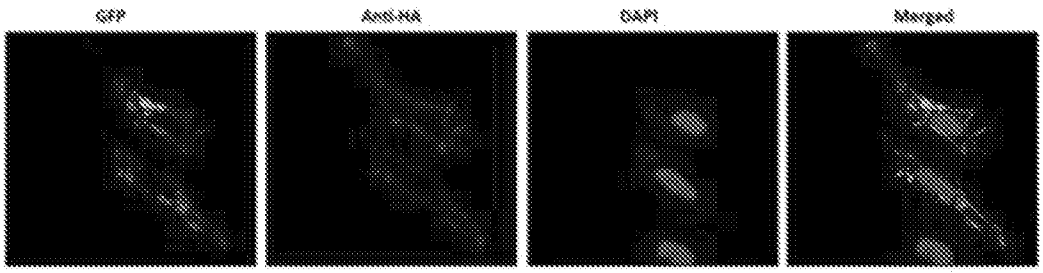

FIG. 6E

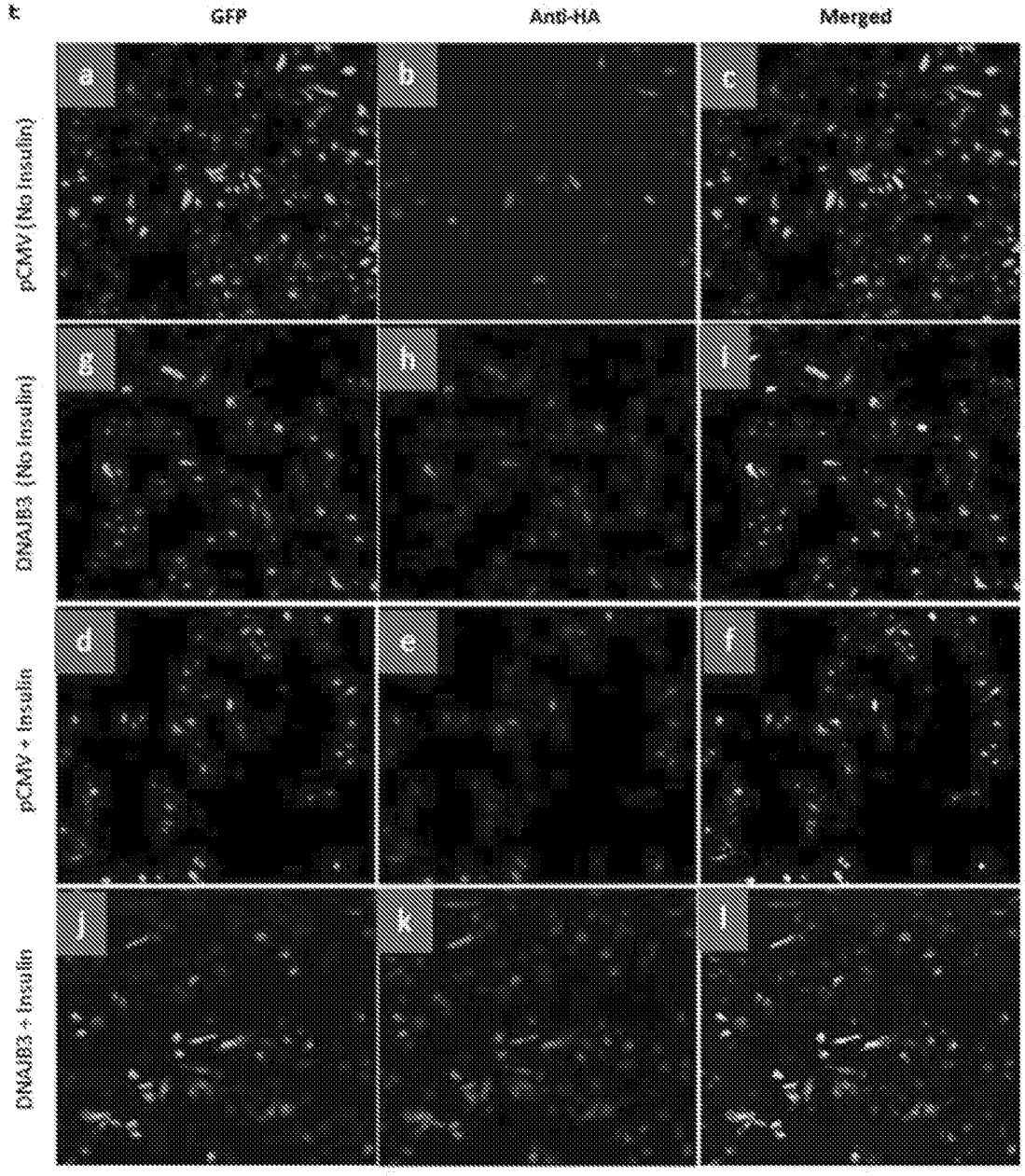
GFP
Anti-HA
Merged
pCMV (No insulin)
DNAJB3 (No insulin)
pCMV + Insulin
DNAJB3 + Insulin
a
b
c
g
h
i
d
e
f
j
k
l

FIG. 6F

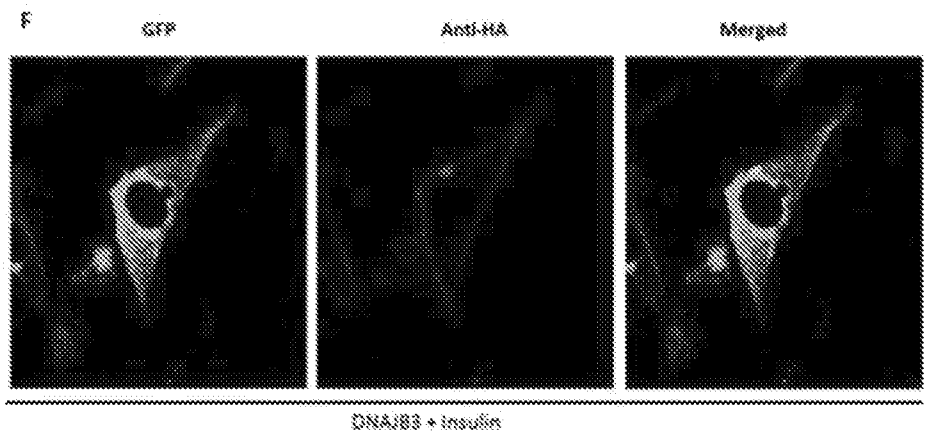
F
GFP
Anti-HA
Merged
DNAJB3 + Insulin

FIG. 6G

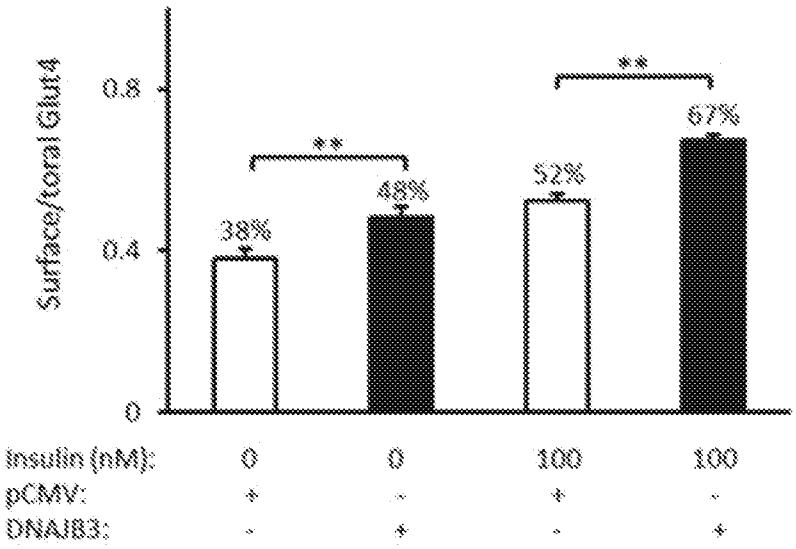
Surface/toral Glut4
0.8
0.4
0
**
**
38%
48%
52%
67%
Insulin (nM): 0 0 100 100
pCMV: + - + -
DNAJB3: - + - +

FIG. 7A

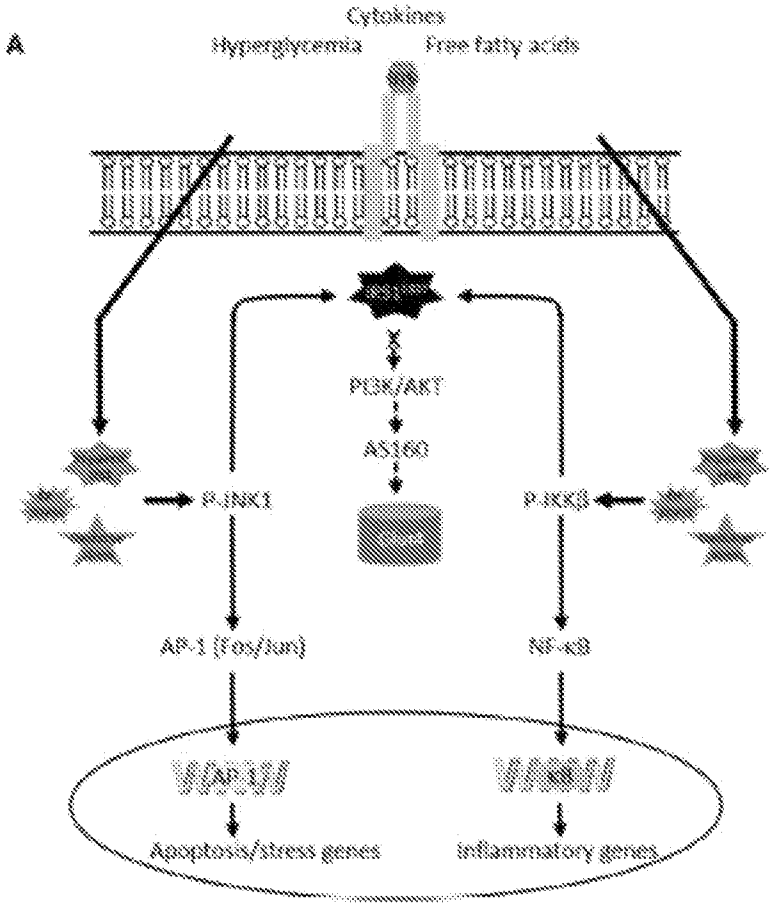
A
Cytokines
Hyperglycemia
Free fatty acids
PI3K/AKT
AS160
P-JNK1
P-IKKβ
AP-1 (Fos/Jun)
NF-κB
Apoptosis/stress genes
Inflammatory genes

FIG. 7B

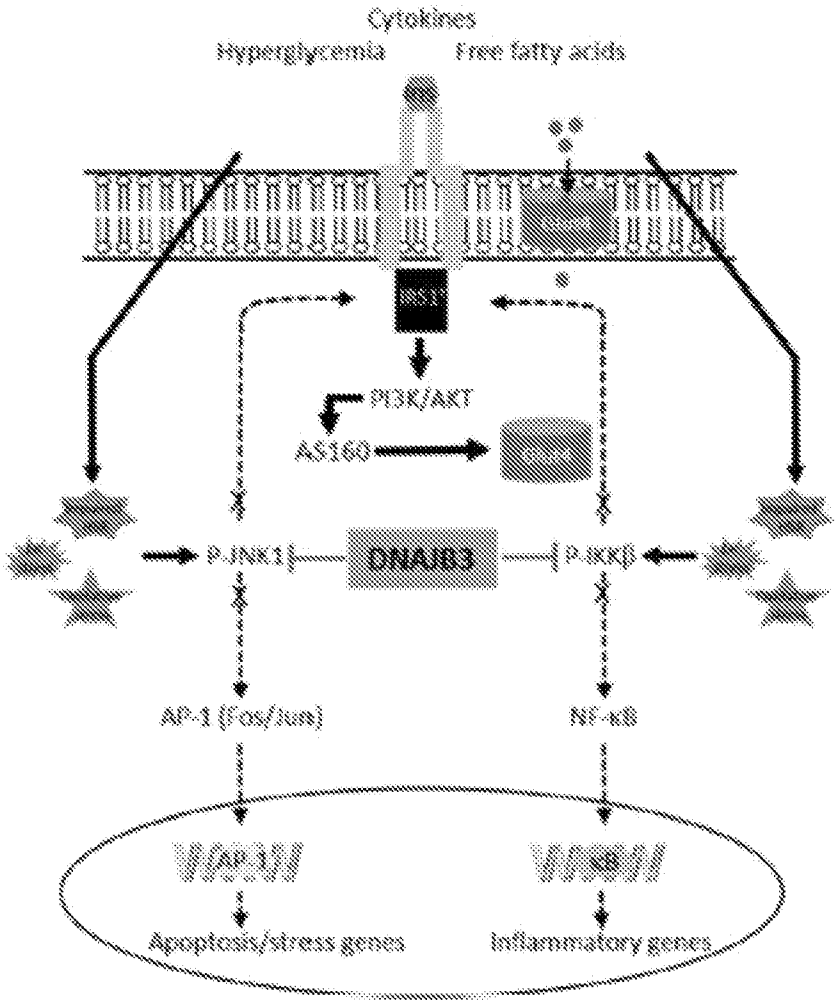
Cytokines
Hyperglycemia
Free fatty acids
IRS1
PI3K/AKT
AS160
P-JNK1
DNAJB3
P-IKKβ
AP-1 (Fos/Jun)
NF-κB
Apoptosis/stress genes
Inflammatory genes

FIG. 8

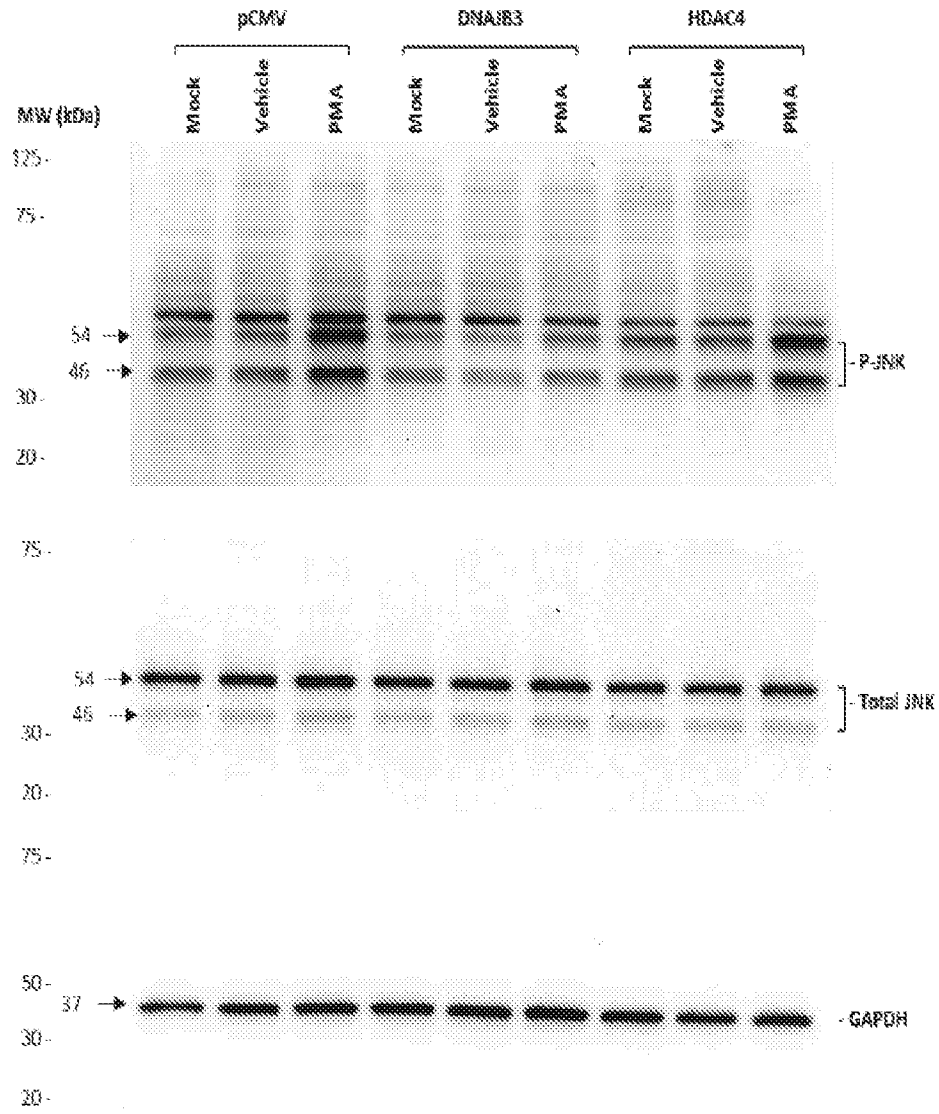
pCMV
DNAJB3
HDAC4
Mock
Vehicle
PMA
MW (kDa)
125
75
54
46
30
20
P-JNK
Total JNK
50
37
GAPDH

FIG. 9

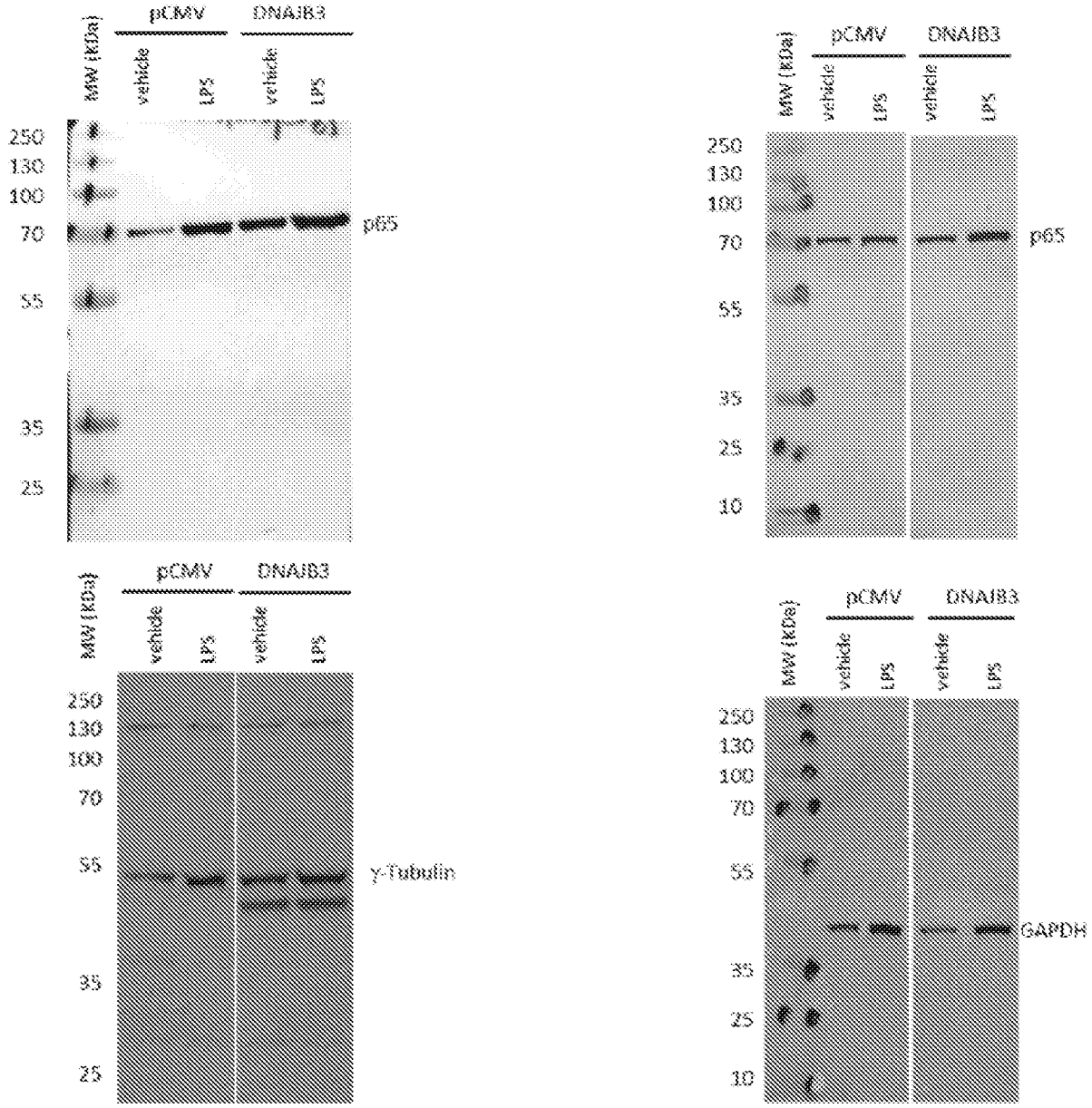
MW (kDa)
pCMV
DNAJB3
vehicle
LPS
250
130
100
70
55
35
25
p65
γ-Tubulin
10
GAPDH

FIG. 10

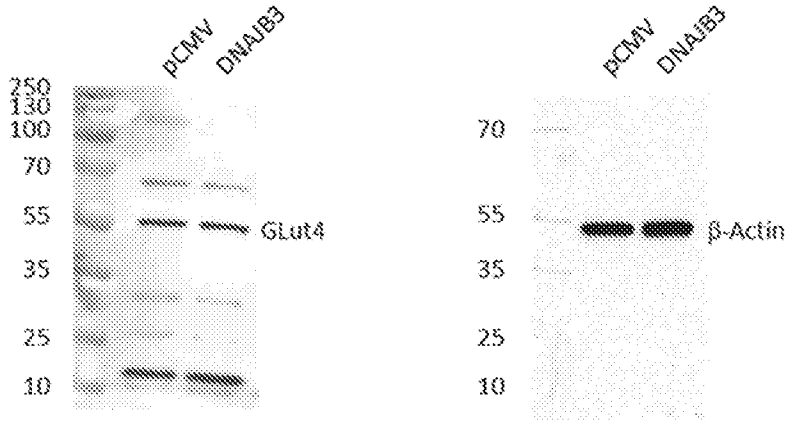

FIG. 11A

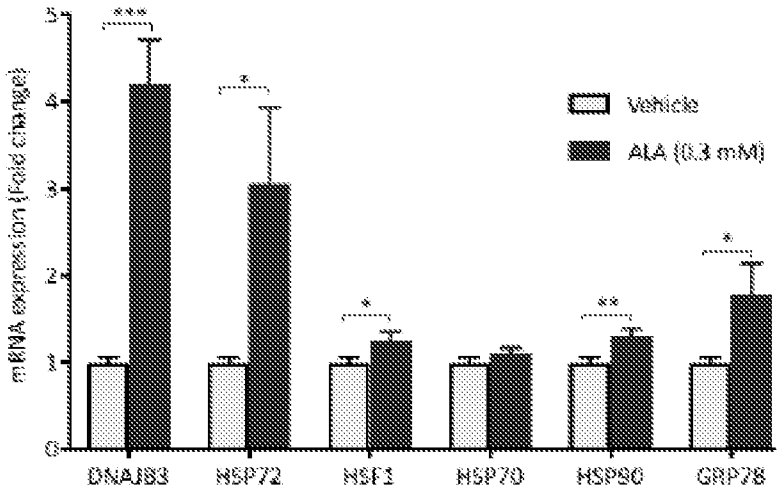

FIG. 11B

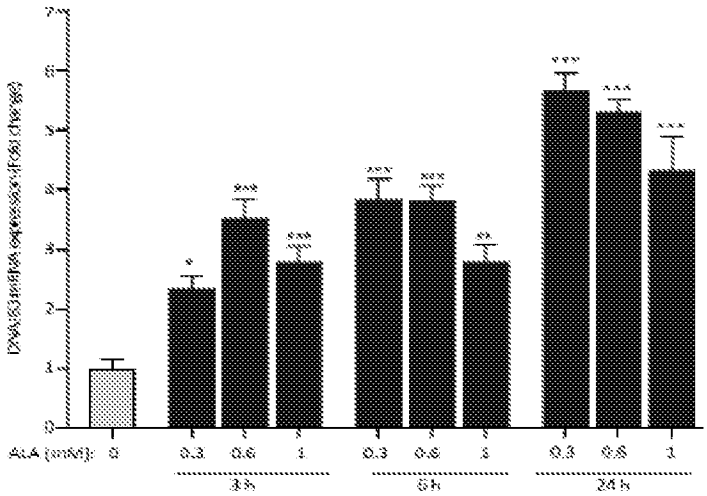

FIG. 11C

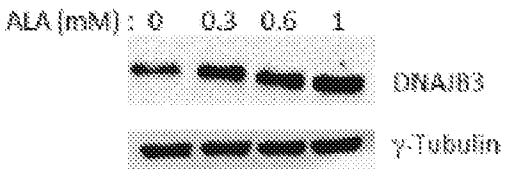

FIG. 11D

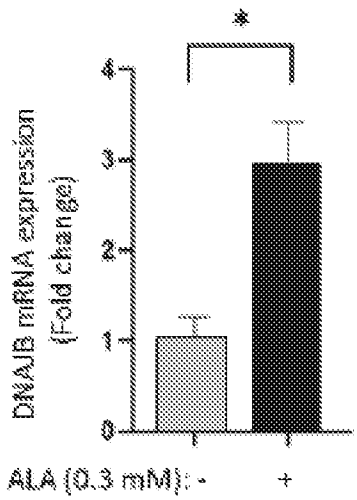

FIG. 11E

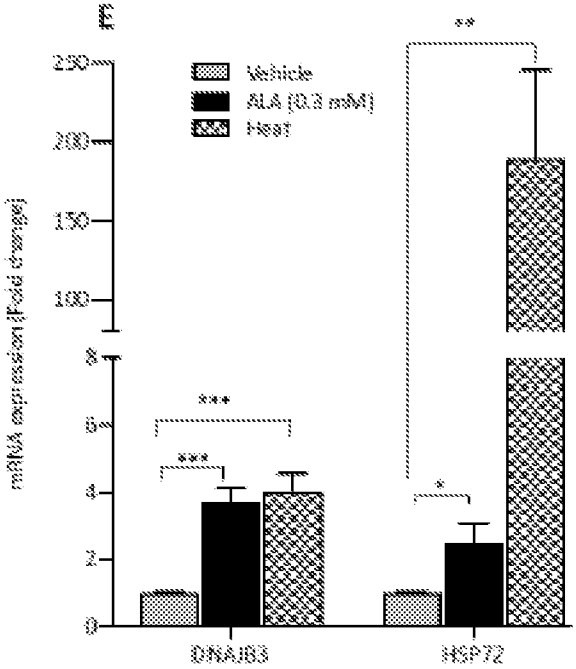

FIG. 12A

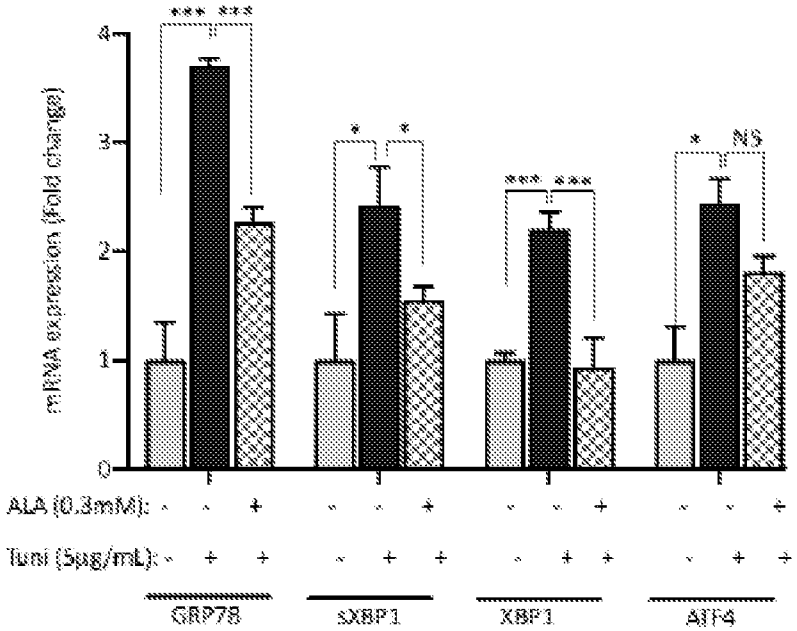

FIG. 12B

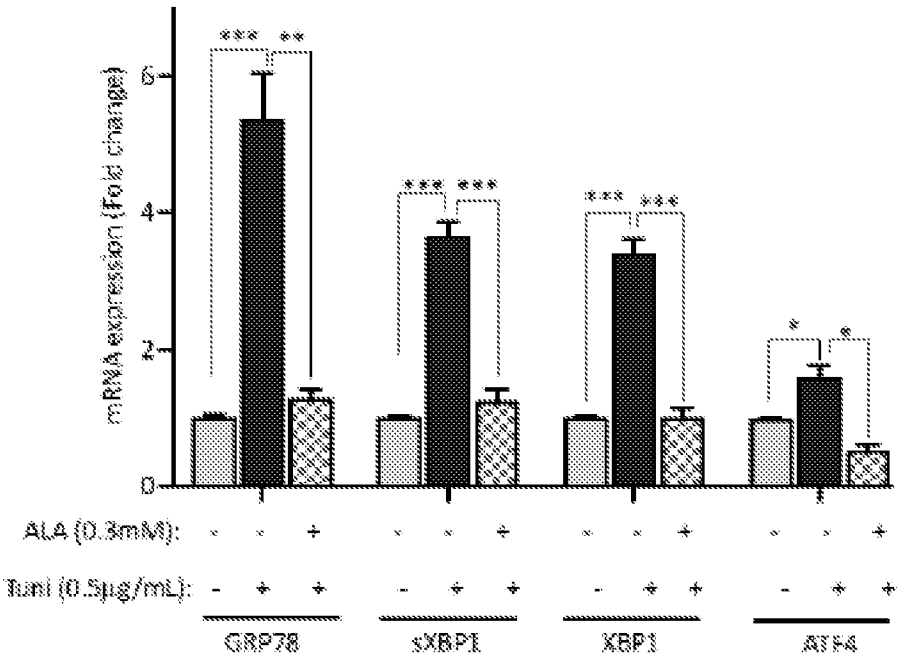

FIG. 12C

FIG. 12D

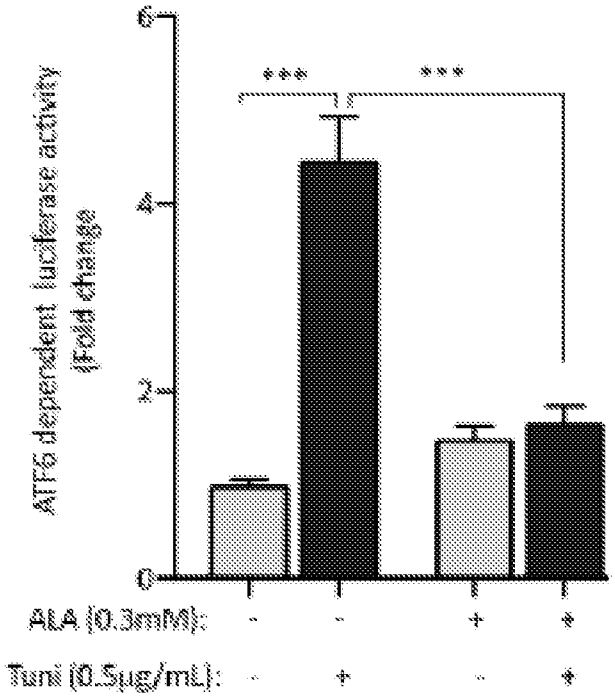

FIG. 12E

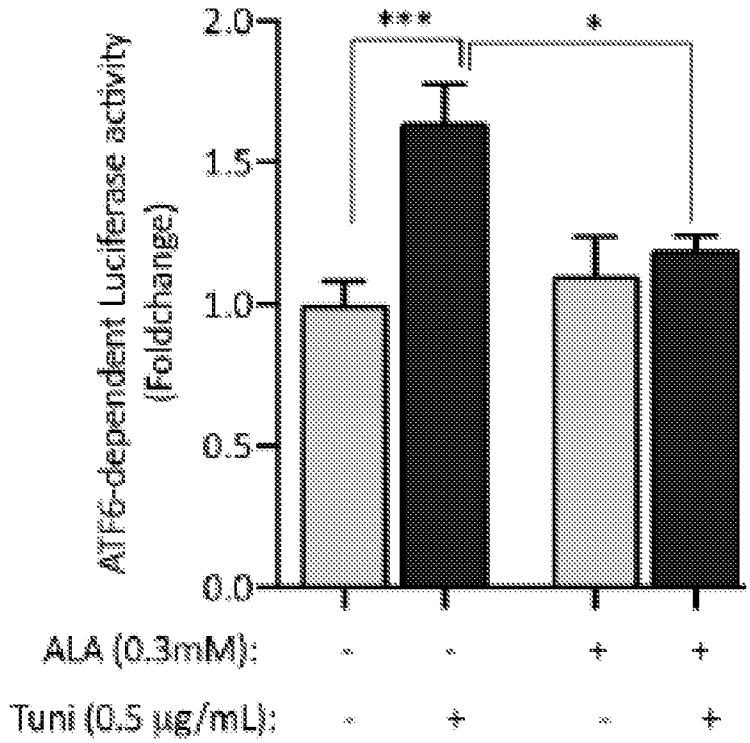

FIG. 13A

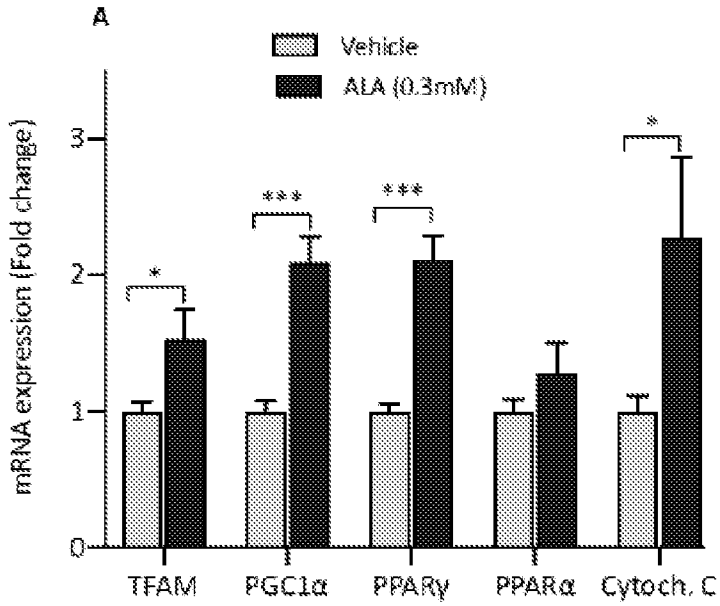

FIG. 13B

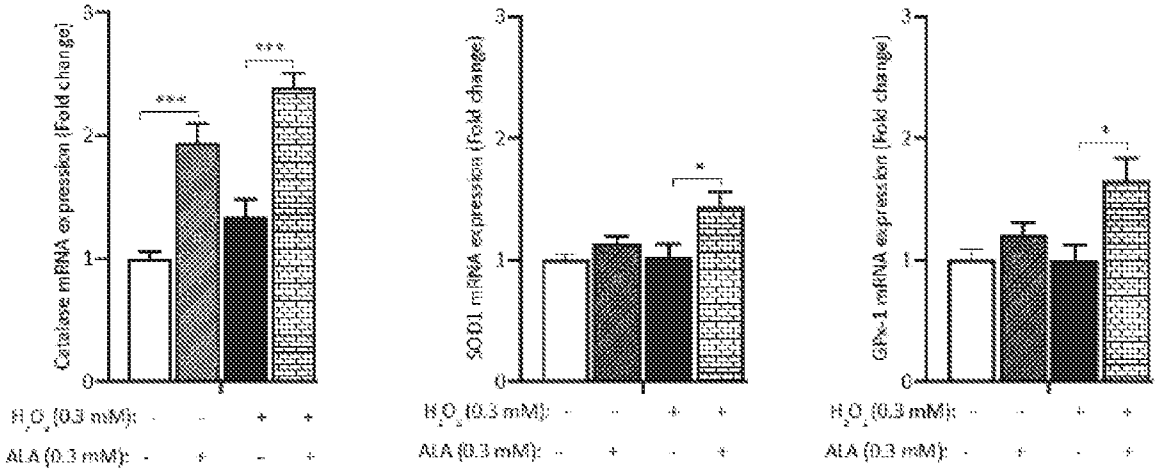

FIG. 14A

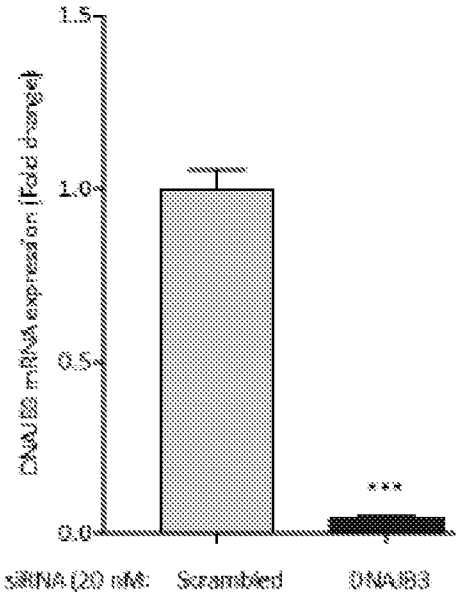

FIG. 14B

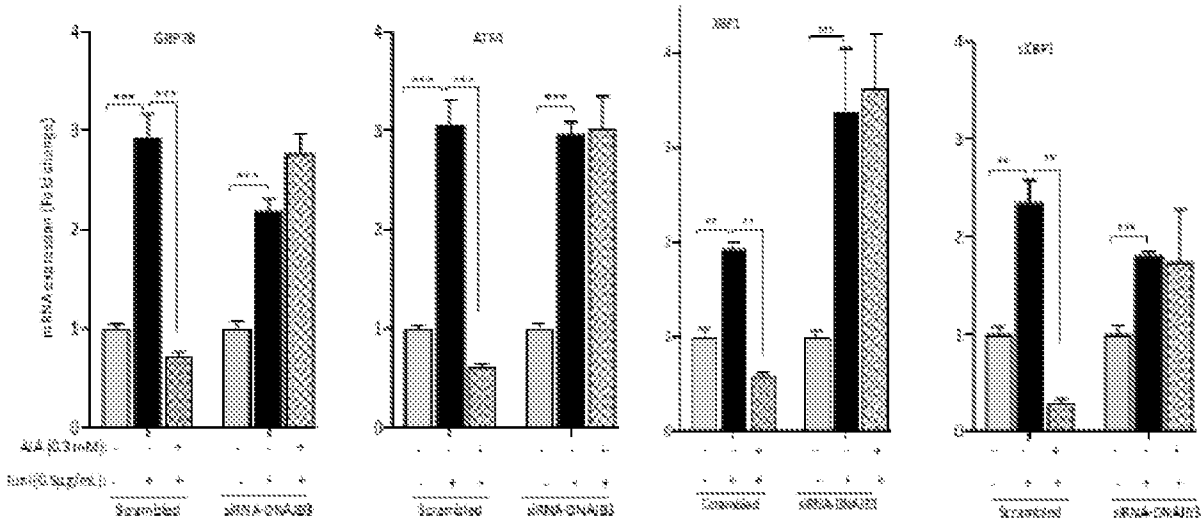

FIG. 14C

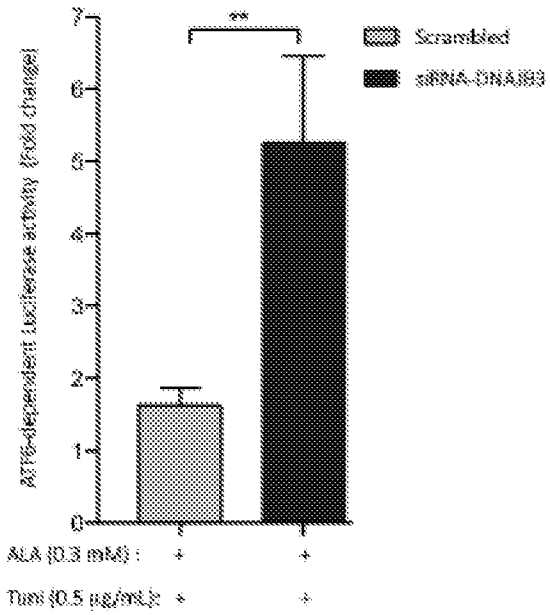

FIG. 15A

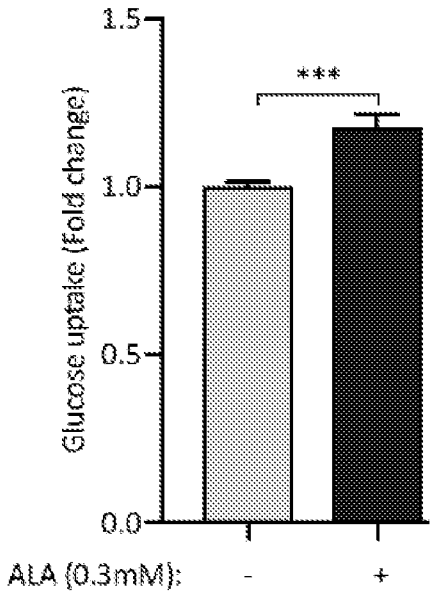

FIG. 15B

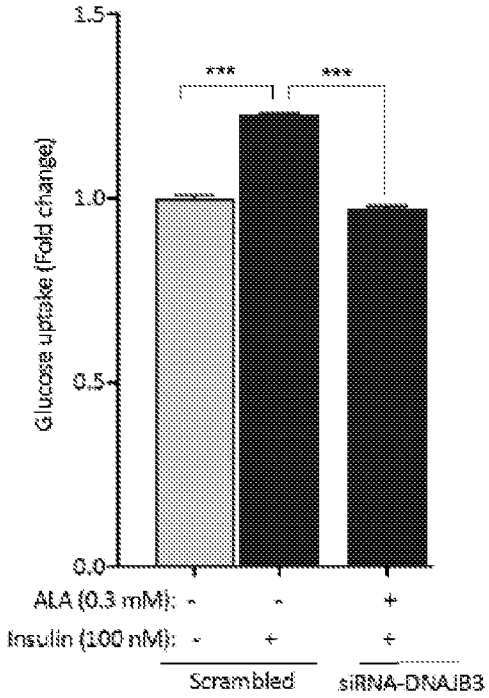

FIG. 16

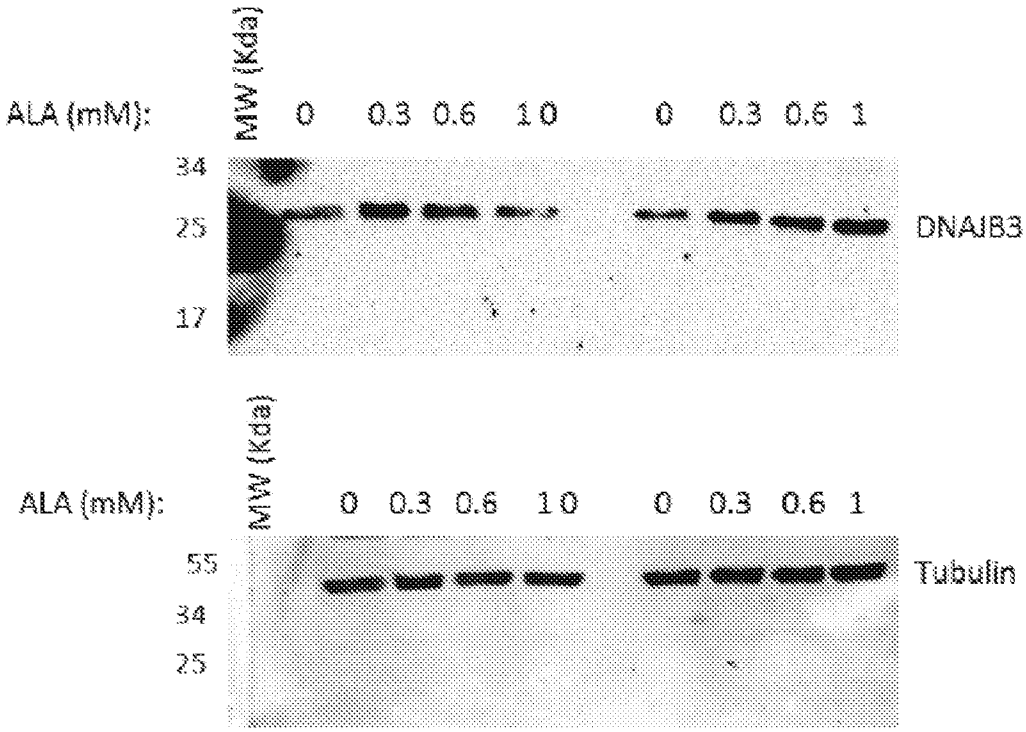
MW (Kda)
ALA (mM):
0 0.3 0.6 1 0 0 0.3 0.6 1
34
25
17
DNAJB3
MW (Kda)
ALA (mM):
0 0.3 0.6 1 0 0 0.3 0.6 1
55
34
25
Tubulin

FIG. 17

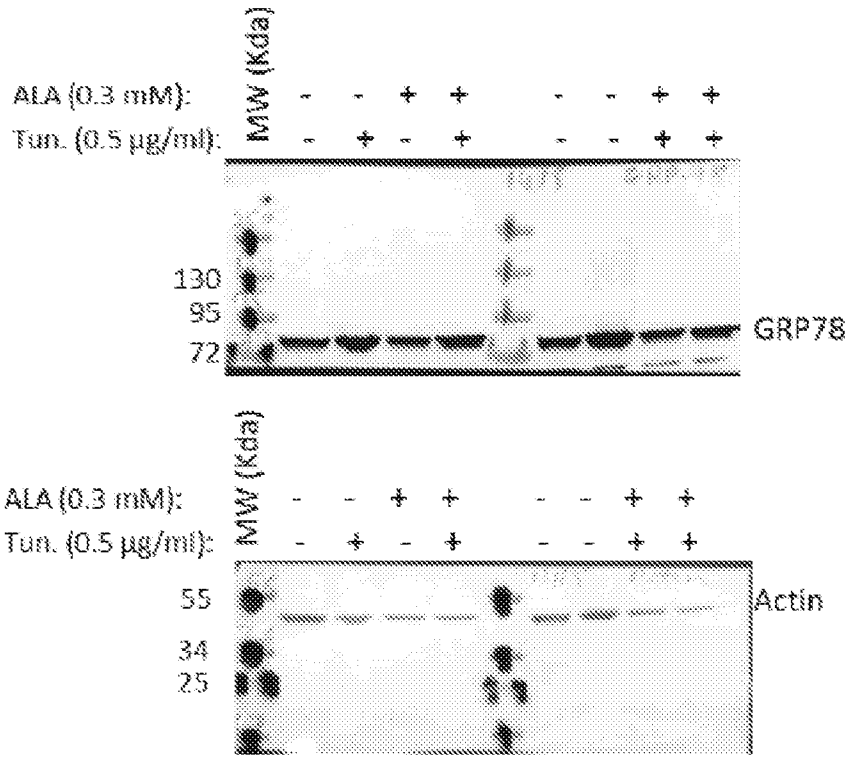

FIG. 18A

Nucleotide sequence of the human DNAJB3 cDNA (438 base pairs)

ATGGTGGACT ACTACGAGGT GCTGGACGTG CCCCGGCAGG CCTCATCCGA
GGCCATCAAG AAGGCGTACC GCAAGCTGGC GCTCAAGTGG CACCCCGACA
AAAACCCTGA GAACAAGGAG GAAGCGGAGA GGAGATTCAA GCAGGTGGCC
GAGGCCTACG AGGTGTTGTC GGACGCCAAG AAACGCGATA TCTATGACCG
CTATGGCGAG GCGGGGGCGG AGGGCGGCTG CACAGGCGGC AGGCCCTTCG
AGGACCCCTT CGAGTACGTC TTCAGCTTCC GCGACCCAGC CGACGTCTTC
AGGGAGTTCT TCGGCGGCCA GGACCCATTC TCCTTTGACC TCTTGGGAAA
CCCGCTGGAG AATATTTTGG GGGGGTCAGA GGAACTGCTG GGGAAGCAGA
AGCAGAGCGT CTGCACCCCT TTTCTCTGCC TTCAGTGA

FIG. 18B

Protein sequence of the human DNAJB3 (145 amino acids).

MVDYYEVLDVPRQASSEAIKKAYRKLALKWHPDKNPENKEEAERR
FKQVAEAYEVLSDAKKRDIYDRYGEAGAEGGCTGGRPFEDPFEYV
FSFRDPADVFREFFGGQDPFSFDLLGNPLENILGGSEELLGKQKQ
SVCTPFLCLQ

FIG. 18C